

A general approach to enhance the survivability of backdoor attacks by decision path coupling

Yufei Zhao
Fudan University
Shanghai, China

Dingji Wang
Fudan University
Shanghai, China

Bihuan Chen*
Fudan University
Shanghai, China

Ziqian Chen
Fudan University
Shanghai, China

Xin Peng
Fudan University
Shanghai, China

ABSTRACT

Backdoor attacks have been one of the emerging security threats to deep neural networks (DNNs), leading to serious consequences. One of the mainstream backdoor defenses is model reconstruction-based. Such defenses adopt model unlearning or pruning to eliminate backdoors. However, little attention has been paid to survive from such defenses. To bridge the gap, we propose VENOM, the first generic backdoor attack enhancer to improve the survivability of existing backdoor attacks against model reconstruction-based defenses. We formalize VENOM as a binary-task optimization problem. The first is the original backdoor attack task to preserve the original attack capability, while the second is the attack enhancement task to improve the attack survivability. To realize the second task, we propose attention imitation loss to force the decision path of poisoned samples in backdoored models to couple with the crucial decision path of benign samples, which makes backdoors difficult to eliminate. Our extensive evaluation on two DNNs and three datasets has demonstrated that VENOM significantly improves the survivability of eight state-of-the-art attacks against eight state-of-the-art defenses without impacting the capability of the original attacks.

1 INTRODUCTION

Deep neural networks (DNNs) have been successfully adopted in a variety of domains, including facial recognition [36, 45], natural language processing [6], and autonomous driving [9]. However, it often requires a large amount of computing resources to train DNNs. To reduce the training cost, it is a common practice for users to directly use models published to model repositories (e.g., Hugging Face), or outsource the model training process to cloud computing platforms (e.g., Google Cloud). While it is cost-efficient to adopt third-party models or third-party platforms, it does introduce security threats.

Backdoor attack has become one of the emerging security threats. Malicious model publishers and untrusted platforms may inject backdoors into DNNs during the training process by poisoning a portion of training samples [25]. The backdoored DNNs misclassify samples with attacker-specified trigger patterns into target labels, while exhibiting normal behavior on benign samples. Many attacks also try to improve the stealthiness of triggers (e.g., [26, 34, 35, 47]). Such attacks can lead to serious consequences. For example, a backdoored

autonomous driving system could classify a stop sign with a particular sticker posted on it as a speed limit sign [10], leading to erroneous decision-making and threatening driver safety. In this work, we focus on image classification, the most popular attacking target.

To mitigate backdoor threats in DNNs, there are two categories of mainstream defenses. *Data distribution-based defenses* (e.g., [2, 46]) assume that models trained on poisoned datasets tend to learn separable latent representations for poisoned and benign samples. Therefore, they identify and eliminate poisoned samples via cluster analysis in the latent space. Instead of focusing on data distribution, *model reconstruction-based defenses* (e.g., [29, 60]) concentrate on model behavior. They are built upon two assumptions, (i) poisoned samples exhibit different activation values in backdoored models from benign samples, and (ii) poisoned samples occupy extra decision paths in backdoored models than benign samples. Therefore, they leverage model unlearning or model pruning to remove backdoors.

In response to advances in defense techniques, previous attacks have achieved progress in improving latent inseparability [37, 41, 55, 61] to bypass data distribution-based defenses. However, little attention has been given to survive from model reconstruction-based defenses. To fill this gap, we propose a *generic* backdoor attack enhancer, VENOM, which enhances existing attacks by improving their *survivability* against existing model reconstruction-based defenses. In general, the key idea of VENOM is to break the two assumptions that those defenses are built upon, making those defenses not applicable. When equipped with VENOM, existing attacks not only preserve their original capabilities (e.g., trigger stealthiness and latent inseparability), but also maintain high attack success rate after those defenses are applied, or in the worst case at least cause a significant decrease in benign accuracy, making the model unusable.

We formulate VENOM as a binary-task optimization problem. The first task is the original backdoor attack task, which aims to preserve the original attack capability, while the second task is the attack enhancement task, which aims to enhance the attack survivability. To realize the second task, we first generate the decision path (a set of neurons) that is crucial for classifying benign samples from a clean model. Then, we propose attention imitation loss to force the decision path of poisoned samples in backdoored models to couple with the generated crucial decision path of benign samples. The coupling is reflected in two dimensions. First, the decision path of poisoned samples overlap with that of benign samples, which breaks the assumption (ii). Second, the activation behavior of poisoned samples is similar to that of benign samples, which breaks the assumption (i). As a result, the backdoor becomes difficult for defense techniques to

*Corresponding Author.

eliminate. Even if certain defense technique successfully eliminates the backdoor, it will inevitably lead to a significant decrease in the classification accuracy of benign samples.

We conduct extensive experiments with two widely used DNN structures (i.e., VGG19-BN [42] and PreActResNet18 [12]) and three popular datasets (i.e., CIFAR-10 [22], CIFAR-100 [22] and GTSRB [13]). We use VGG19-BN for all the three datasets, and PreActResNet18 for the CIFAR-10 dataset. We evaluate eight state-of-the-art backdoor attacks, i.e., BadNets [10], Blend [3], TrojanNN [31], LC [47], SSBA [26], Inputaware [34], WaNet [35] and Adap-Blend [37], and eight state-of-the-art backdoor defenses, i.e., FT [29], NAD [28], I-BAU [57], NC [53], BNP [60], FP [29], CLP [59], NPD [62].

We first measure how VENOM affects the capability of the original attacks when no defense is applied. On average, VENOM slightly improves the attack success rate of the eight original attacks by 2.45% at the cost of a slight decrease of the benign accuracy by 0.30%. Hence, VENOM preserves the capability of existing backdoor attacks. Then, we measure how VENOM affects the survivability of the original attacks when various defenses are applied. On average, VENOM significantly enhances the original attacks’ survivability from 39.10% to 62.45%.

Finally, we explore the factors that impact the performance of VENOM, and adopt explainability techniques to delve into the intrinsic mechanism of VENOM, explaining the performance of VENOM.

In summary, this work makes the following main contributions.

- We have proposed VENOM, the first generic approach to enhance the survivability of existing backdoor attacks against existing model reconstruction-based backdoor defenses.
- We have conducted large-scale experiments with eight backdoor attacks and eight backdoor defenses to demonstrate that VENOM significantly improves the survivability of attacks against defenses without impacting the capability of the original attacks.
- We have implemented VENOM and released the source code of VENOM at <https://github.com/VenomEnhancer/Venom>.

2 RELATED WORK

We review the most closely relevant works in two aspects, i.e., backdoor defenses and attacks. We refer readers to recent surveys [8, 19, 25] for a comprehensive discussion about the state-of-the-art.

2.1 Backdoor Defenses

Several backdoor defenses have been proposed to mitigate backdoor threats in DNNs. Mainstream defenses include two categories, i.e., data distribution-based and model reconstruction-based defenses. Data distribution-based defenses are built upon the assumption that models trained on poisoned datasets tend to learn highly distinct latent representations for poisoned and benign samples in the target class, forming two distinct clusters in various latent spaces. For example, Tran et al. [46] and Chen et al. [2] propose to identify and remove poisoned samples via cluster analysis in the latent space, and retrain the model with the remaining samples. Hayase et al. [11] and Tang et al. [44] improve the previous two approaches to work well even at a low poison rate. However, several attacks [41, 55, 61] have shown resistance against such data distribution-based defenses.

Model reconstruction-based defenses are usually based on two assumptions as detailed in Section 1, and use backdoor unlearning and

pruning to mitigate the threats. Given the first observation, defenders leverage unlearning to correct model’s activation behavior. For example, Liu et al. [29] fine-tune the backdoored model on a subset of benign samples, leveraging the catastrophic forgetting of DNNs to forget the backdoor. Zeng et al. [57] formulate the unlearning as a mini-max problem, and propose implicit backdoor adversarial unlearning to solve the problem. Li et al. [28] adopt knowledge distillation to reconstruct the backdoored model. Wang et al. [53] first synthesize the potential trigger and determine the target class, and then exploit this knowledge to unlearn the backdoor.

Given the second observation, defenders identify the neurons or channels in backdoor-related decision paths and prune them. For example, Liu et al. [29] propose to prune neurons that are dormant for benign samples because neurons associated with backdoor-related behavior often remain inactive when processing benign samples, and combine pruning with fine-tuning to strengthen the defense. Zheng et al. [59, 60] observe that the standardized entropy of backdoor-related neurons is significantly lower than clean neurons, and channels with high Lipschitz constants is backdoor-related, and hence they prune such neurons or channels to remove the backdoor. Inspired by the mechanism of the optical polarizer, Zhu et al. [62] insert a learnable neural polarizer into the backdoored model as an intermediate layer, filtering trigger information and therefore blocking the subsequent backdoor-related decision paths.

There also exist several other defenses. Certified defenses are often based on random smoothing techniques [52] or ensemble techniques [17, 18, 24] to provide a theoretical guarantee under certain assumptions. However, they are generally weaker than the above empirical defenses in practice [25]. Poison suppression-based defenses [14, 27] attempt to prevent the creation of hidden backdoors by depressing the effectiveness of poisoned samples during the training process. However, they assume that defenders have control over the training process. Preprocessing-based defenses [7, 32, 48, 51] use trigger override or data augmentation to prevent the backdoor from being activated in the inference phase. However, they focus on attacks that use local patches as triggers, and thus are less applicable to defend a wide range of attacks.

2.2 Backdoor Attacks

Gu et al. [10] introduce the first backdoor attack, named BadNets, in DNNs. It generates poisoned samples by simply stamping the fixed backdoor trigger onto the selected benign samples and changing their labels to attacker-specified target labels, and hence it is considered as a *poison-label visible attack*. Since then, various similar backdoor attacks have been proposed. For example, Chen et al. [3] propose to blend instead of stamp the fixed backdoor trigger with benign samples; and Liu et al. [31] propose to generate a general trojan trigger by inverting the neural network.

Specifically, one thread of works attempt to achieve *clean-label attacks*, where the poisoned samples are not mislabeled but correctly labeled to evade label inspection. For example, Turner et al. [47] propose to poison the benign samples via adversarial perturbations and generative models with the goal of rendering them hard to classify and keeping the modification small to ensure the consistent label. Another thread of works try to realize *sample-specific attacks*, where

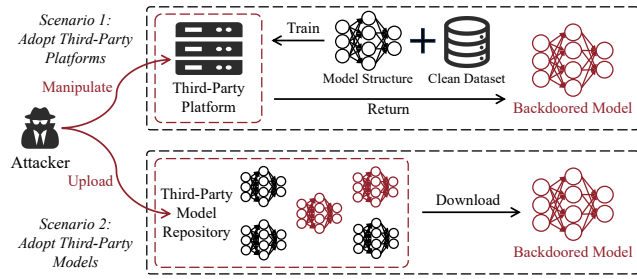


Figure 1: The threat model of VENOM on two typical scenarios. During the backdoor injection, the attacker can only control the pipeline within the attacker’s capabilities (red areas), but cannot change any victim’s behaviors (black areas).

different poisoned samples have different backdoor triggers. For example, Nguyen and Tran [34] argue that fixed triggers are easily detected, and propose the first sample-specific backdoor attack. They develop an input-aware trigger generator driven by diversity loss. To further make the sample-specific triggers invisible and improve the stealthiness, Nguyen and Tran [35] use image warping to inject backdoor triggers, and Li et al. [26] use DNN-based image steganography to generate invisible sample-specific backdoor triggers.

With the advancement of backdoor defense techniques, backdoor attacks have started to focus on the resistance against backdoor defenses. Several techniques [41, 55, 61] have been proposed to reduce the latent separation between poisoned and benign samples, thus circumventing existing data distribution-based defenses. However, these attacks assume additional control over the training process. Instead, Qi et al. [37] reduce the latent separation in poison-only attacks which only assume control over a small part of training data.

In summary, the existing attacks merely focus on optimized trigger and data distribution, but barely consider the resistance to model reconstruction-based defenses. Our work fills this gap by developing a generic enhancer that not only improves the survivability of the existing attacks against various model reconstruction-based defenses but also preserves the existing attacks’ original characteristics (e.g., trigger stealthiness and latent inseparability).

3 THREAT MODEL

Attacker’s Goals. The attacker aims to enhance existing backdoor attacks to craft a backdoored model that achieves three goals.

- *Effectiveness Goal.* The backdoored model should predict the poisoned sample with the specific trigger as the target label.
- *Utility Goal.* The backdoored model should maintain the same predictive power as a clean model on benign samples.
- *Survivability Goal.* The backdoored model should survive from existing model reconstruction-based defenses. Specifically, after taking defensive measures, the backdoored model should still be able to achieve the effectiveness goal, or at least fail to achieve the utility goal (i.e., making the backdoored model unusable).

Attacker’s Capabilities. As a generic backdoor attack enhancement technique, attacker’s capabilities should be applicable to most attacks. We consider the following two typical scenarios where backdoor threats could occur [25], as shown in Figure 1.

- *Scenario 1: Adopt Third-Party Platforms.* Users provide their clean dataset, model structure, and training schedule to a potentially untrusted third-party platform (e.g., Google Cloud) to train their model. The attacker can hack into the platform (or the attacker is the service provider of the platform), and can manipulate the clean dataset and training schedule to inject the backdoor. However, the attacker cannot change the model structure; otherwise, users will be aware of the change and notice the attack. After training, users will get the backdoored model from the platform.
- *Scenario 2: Adopt Third-Party Models.* The attacker can upload the backdoored model to any third-party model repository (e.g., Hugging Face). In that sense, the attacker can have the full access to the whole training process, including the dataset, model structure, and training schedule.

Defender’s Capabilities. In both scenarios, the defender cannot control the training process, but can modify the backdoored model. In Scenario 1, the defender can also access the clean dataset.

4 METHODOLOGY

We first formalize backdoor attack enhancer VENOM, then introduce the overview of VENOM, and finally elaborate each step of VENOM.

4.1 Formalization of VENOM

We first formalize VENOM as a bi-level optimization problem, and then formalize VENOM as a binary-task optimization problem.

Bi-Level Optimization Problem. In classic DNN training, a clean model $f : \mathcal{X} \rightarrow \mathcal{Y}$ is trained on a clean dataset \mathcal{D}_c to fit the data distribution $\mathcal{X} \times \mathcal{Y}$, where \mathcal{X} denotes the input space, \mathcal{Y} denotes the output space representing class labels, and \mathcal{D}_c denotes a set of data samples $(x, y) \in \mathcal{X} \times \mathcal{Y}$. To achieve the attacker’s goals, the attacker needs to inject a backdoor into the clean model f to generate a backdoored model f' which is trained on a backdoored dataset \mathcal{D}_{bd} . The backdoored dataset \mathcal{D}_{bd} is generated by poisoning a certain rate of data samples in the clean dataset \mathcal{D}_c . The data poisoning maps samples with the backdoor trigger τ to the target label t , with the poisoned sample generator $\mathcal{G} : \mathcal{X} \rightarrow \mathcal{X}$ and the label flipper $\mathcal{F} : \mathcal{X} \times \mathcal{Y} \rightarrow \mathcal{Y}$. $\mathcal{J} = \{j_1, \dots, j_k\}$ denotes the indices of the k poisoned samples, and these poisoned samples are denoted as \mathcal{D}_{bd}^p . The remaining samples are benign samples, denoted as \mathcal{D}_{bd}^b . Therefore, $\mathcal{D}_{bd} = \mathcal{D}_{bd}^p \cup \mathcal{D}_{bd}^b$, and each data sample $(x'_i, y'_i) \in \mathcal{D}_{bd}$ is formulated by Eq. 1.

$$x'_i = \begin{cases} \mathcal{G}(x_i), & i \in \mathcal{J} \\ x_i, & \text{otherwise} \end{cases}, \quad y'_i = \begin{cases} \mathcal{F}(x_i, y_i), & i \in \mathcal{J} \\ y_i, & \text{otherwise} \end{cases} \quad (1)$$

We design VENOM as a generic backdoor attack enhancer, and formalize it as a bi-level optimization problem, as formulated by Eq. 2,

$$\begin{aligned} \min \quad & \mathcal{L}_{out}(\mathcal{D}_{bd}, f'^*) = \sum_{(x', y')}^{\mathcal{D}_{bd}} \mathbb{I}(f'^*(x') \neq y'), \\ \text{s.t.} \quad & f'^* \in \arg \min_{f'} \mathcal{L}_{inner}(\mathcal{D}_{bd}[t], f, f'), \\ \text{where} \quad & \mathcal{L}_{inner} = \sum_{(x', y')}^{\mathcal{D}_{bd}[t]} \mathcal{S}(x', x_{ref}, f', f) \end{aligned} \quad (2)$$

where $\mathbb{I}(\cdot)$ denotes the indicator function, i.e., $\mathbb{I}(\cdot) = 1$ if \cdot is true and $\mathbb{I}(\cdot) = 0$ if \cdot is false; $\mathcal{D}_{bd}[t]$ denotes the set of samples with the target label t in \mathcal{D}_{bd} , including both benign and poisoned samples; x_{ref} denotes a reference sample with the target label t , which is randomly selected from \mathcal{D}_c ; and \mathcal{S} denotes a similarity function.

In outer optimization, we minimize the loss function \mathcal{L}_{out} , which measures the number of samples that are not predicted as the corresponding label y' by the optimal backdoored model f'^* . Specifically, \mathcal{L}_{out} not only forces f'^* to predict the correct label y' for each benign sample, which satisfies the attacker's utility goal, but also forces f'^* to identify the trigger τ and predict the target label t for each poisoned sample, which satisfies the attacker's effectiveness goal.

In inner optimization, we minimize the loss function \mathcal{L}_{inner} to find the optimal backdoored model f'^* which satisfies the attacker's survivability goal. To this end, we force the decision paths and activation values of both poisoned and benign samples in $\mathcal{D}_{bd}[t]$ in the backdoored model f' to be similar to those of reference samples in the clean model f . Hence, poisoned samples and benign samples in $\mathcal{D}_{bd}[t]$ have similar decision paths and activation values in f' , which breaks the assumptions of existing model reconstruction-based defenses and thus makes f' survive from those defenses.

Binary-Task Optimization Problem. It is difficult to guarantee the optimal solution for the bi-level optimization problem, and only strong stationary solution can be obtained [30]. Moreover, the solving process is complicated and requires prohibitive time overhead. Therefore, we relax it into a binary-task optimization problem to find an approximate solution, using the joint loss function in Eq. 3,

$$\mathcal{L} = \omega_1 \cdot \mathcal{L}_1 + \omega_2 \cdot \mathcal{L}_2 \quad (3)$$

where \mathcal{L}_1 is the loss function of the first task, i.e., the *original backdoor attack task*, \mathcal{L}_2 is the loss function of the second task, i.e., the *attack enhancement task*, and ω_1 and ω_2 are the weight to each task.

In the first original backdoor attack task, VENOM aims to preserve the original attack capability, i.e., to inject a backdoor and satisfy the effectiveness and utility goals. This corresponds to the outer optimization in bi-level optimization. Existing backdoor attacks can be unified into the minimization of the loss function \mathcal{L}_1 in Eq. 4,

$$\mathcal{L}_1 = \sum_{(x', y')}^{\mathcal{D}_{bd}} l(x', y', f') + l_{tc} \quad (4)$$

where the loss $l(x', y', f')$ measures the difference between the backdoored model's predicted label $f'(x')$ and the ground truth label y' . In multi-classification, the cross-entropy loss is commonly adopted as l . Apart from data poisoning, some backdoor attacks also control the training phase and introduce the additional loss l_{tc} , which we also inherit to keep the capability of original backdoor attacks.

In the second attack enhancement task, VENOM aims to enhance the attack survivability from model reconstruction-based defenses, i.e., to satisfy the survivability goal. This corresponds to the inner optimization in bi-level optimization. The loss function \mathcal{L}_2 of this task will be introduced in Section 4.5.

4.2 Overview of VENOM

Based on the formalization of the binary-task optimization, we present the approach overview of VENOM in Figure 2. Specifically, VENOM first conducts *micro-training*, i.e., training the model on the clean dataset

for a few epochs. The resulting micro-trained model will be used to initialize the model in backdoor injection and enhancement. Then, it finishes the training on the clean dataset to obtain a clean model, and conducts *target crucial decision path generation* to produce the decision path (i.e., a set of neurons) that is crucial for classifying benign samples with the target label from a clean model. Finally, it conducts *binary-task training* to inject backdoor and enhance attack survivability. For the original backdoor attack task, it uses the original loss, as formulated in Section 4.1. For the attack enhancement task, it uses a novel *attention imitation loss* to force the decision path of poisoned samples in the backdoored model to couple with the generated crucial decision path of benign samples with the target label. This coupling ensures that the behavior of our enhanced backdoored model is closely similar to that of the clean model, thereby enabling it to survive from existing model reconstruction-based defenses. In the following sections, we present the three key steps: micro-training, target crucial decision path generation, and binary-task training.

4.3 Micro-Training

In the micro-training step, we train the model on the clean dataset for a few epochs (e.g., 5% of the whole epochs). This resulting early-stage clean model, referred to as a micro-trained model f_m , already exhibits some level of performance, but has not fully learned the features from the clean dataset. Instead of training the enhanced backdoored model from scratch in the later binary-task training step (see Section 4.5), we utilize this micro-trained model as the initialization. This design is inspired by task scheduling in multi-task learning [16]. Micro-training helps VENOM to establish basic model classification capability and feature representations before introducing the backdoor attack task and attack enhancement task.

Specifically, micro-training mainly plays two roles. First, it guides the overall direction of our binary-task optimization. The two tasks exhibit significant differences in complexity, with the more complex backdoor attack task dominating the optimization direction. If the model is initialized randomly, this dominance results in premature overfitting to the backdoor attack task, while the attack enhancement task fails to be effectively trained. Our micro-training reduces the learning complexity of the backdoor attack task, as it shares similarities with the learning objective of the backdoor attack task. Consequently, it to some extent balances the complexity and learning speed of the two tasks. In this way, the overall optimization direction does not excessively favor the backdoor attack task, preventing the model from getting stuck in local optima, and instead follows a more balanced direction. Second, it facilitates the inclination of the enhanced backdoored model in binary-task optimization towards the clean model's behavior, which also contributes to enhancing the model's survivability to some extent.

4.4 Target Crucial Decision Path Generation

Given a clean model, this step aims to generate the decision path that is crucial for classifying benign samples with the target label. Such a decision path is referred to as target crucial decision path (TCDP). Typically, decision path is composed of neurons (e.g., convolutional kernels in a CNN). According to the literature on DNN [20], the shallow layers of the network extract abstract features from the samples, while the deep layers are capable of extracting specific features from

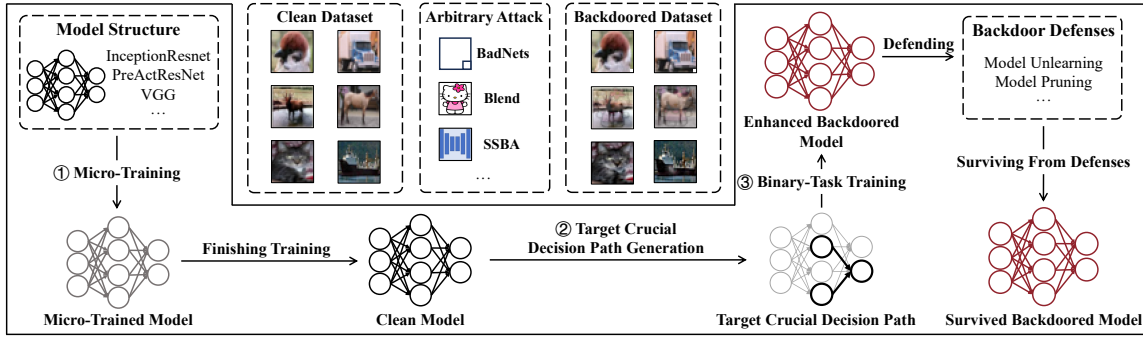


Figure 2: Approach overview of VENOM.

Algorithm 1 Target Crucial Decision Path Generation

Require: clean model f , neurons in a selected layer N_{layer} , clean dataset \mathcal{D}_c , target class t , total number of neurons in the TCDP k

Ensure: a set of neurons that form the TCDP \mathcal{N}

```

1:  $\triangleright$  Select crucial neurons for each class
2: for each class  $i$  do
3:    $S_i \leftarrow \text{CALCSIMILARITY}(f, N_{layer}, \mathcal{D}_c[i])$ 
4:    $\mathcal{N}_i \leftarrow \{n \mid S_i[n] > \epsilon_1\}$ 
5:  $\triangleright$  Remove common neurons
6:  $S_t \leftarrow \text{CALCSIMILARITY}(f, N_t, \mathcal{D}_c)$ 
7:  $\mathcal{N}_t \leftarrow \{n \mid n \in \mathcal{N}_i \text{ and } S_t[n] < \epsilon_2\}$ 
8:  $\triangleright$  Select neurons that form the TCDP
9: for each neuron  $n \in \mathcal{N}_t$  do
10:   $\lfloor$   $\text{Count}[n] \leftarrow$  the number of classes that consider  $n$  as crucial
11:  $\mathcal{N} \leftarrow$  top  $k$  neurons in  $\mathcal{N}_t$  sorted by  $\text{Count}$ 
12: return  $\mathcal{N}$ 
13: function  $\text{CALCSIMILARITY}(f, N_{candidate}, \mathcal{D})$ 
14:    $S \leftarrow \emptyset$ 
15:    $\mathcal{D}^a, \mathcal{D}^b \leftarrow$  divide  $\mathcal{D}$  into two groups randomly
16:   for each neuron  $n \in N_{candidate}$  do
17:      $s \leftarrow 0$ 
18:      $\triangleright$  Calculate the similarity of each sample pair
19:     for each sample pair  $(x_a, x_b) \in \mathcal{D}^a \times \mathcal{D}^b$  do
20:        $s \leftarrow s + \text{sim}(\sigma_n(x_a, f), \sigma_n(x_b, f))$ 
21:      $S[n] \leftarrow s / (\text{size}(\mathcal{D}^a) * \text{size}(\mathcal{D}^b))$ 
22:   return  $S$ 

```

the samples. Therefore, we select neurons in a single deep layer as candidate neurons, from which we further calculate the TCDP.

After determining the single deep layer, we select a fixed number of neurons to form the TCDP. We select neurons that exhibit similar activation values for benign samples with the target label, meaning that they are crucial for the classification of the target class. Further, we exclude common neurons which have similar activation values across all sample classes and thus are not crucial for classification. We also favor neurons that also play important roles in classification of some other classes. Our selection aims to couple the decision path of poisoned samples with that of benign samples from multiple classes in binary-task training (see Section 4.5), thereby increasing the difficulty and cost of implementing effective defenses.

Algorithm 1 shows the procedure to generate the TCDP. First, for each class i , it computes the similarity of activation values of samples in this class $\mathcal{D}_c[i]$ on all neurons N_{layer} in a selected layer (Line 2-3) through the CALCSIMILARITY function (Line 13-22). Specifically, this function first randomly divides the dataset \mathcal{D} into two groups

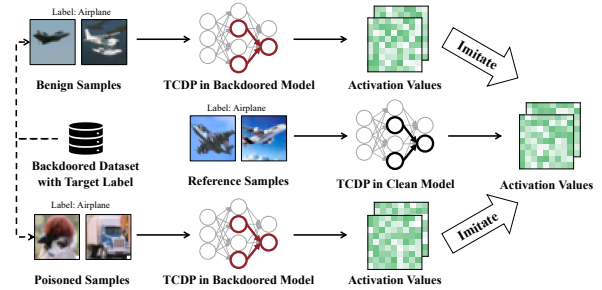


Figure 3: Illustration of attention imitation loss.

\mathcal{D}^a and \mathcal{D}^b (Line 15), then computes the cosine similarity $\text{sim}(\cdot, \cdot)$ of the activation values $\sigma_n(\cdot, \cdot)$ of each sample pair (x_a, x_b) on each candidate neuron n (Line 19-20), and finally calculates the average activation value similarity of each sample pair on each neuron (Line 21). Next, for each class i , Algorithm 1 proceeds to select crucial neurons \mathcal{N}_i (Line 4), which consists of neurons exhibiting an average activation value similarity greater than the threshold ϵ_1 .

Next, Algorithm 1 computes the similarity of activation values of the samples from the entire clean dataset \mathcal{D}_c on the crucial neurons of the target class \mathcal{N}_t (Line 6), and removes the common neurons whose activation value similarity across the entire clean dataset exceeds the threshold ϵ_2 (Line 7). In other words, the removed common neurons exhibit similar activation behavior for all classes.

Finally, Algorithm 1 sorts each crucial neuron n in \mathcal{N}_t based on the number of classes whose crucial neurons also contain n , meaning that n is also important for some other classes, and selects the top k neurons \mathcal{N} to form the TCDP (Line 9-11).

4.5 Binary-Task Training

The binary-task training step involves two tasks. The first task is to inject backdoor, which uses the loss of the original backdoor attack as formulated in Eq. 4. The second task is to enhance attack survivability, which uses our novel attention imitation loss. We also optimize the binary-task training to better balance the two tasks.

Attention Imitation Loss. To make a backdoor attack survive from defenses, our goal is to force the behavior of poisoned samples in the backdoored model to imitate that of benign samples. To achieve this goal, we introduce a novel *attention imitation loss*. It is inspired by attention transfer loss [56], but involves two adaptations. First, we refine the computation granularity to the level of neurons instead of the layer level in attention transfer loss, which enables more

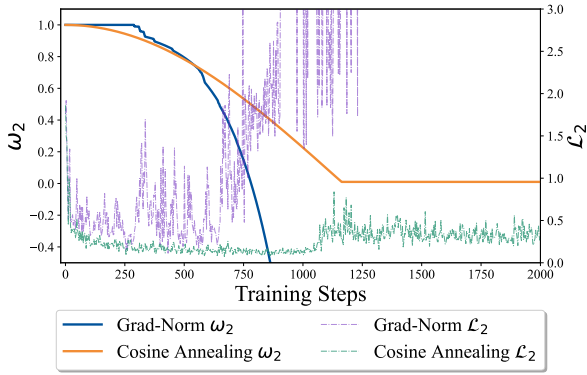


Figure 4: Training process using different strategy.

precise control over activation values. Besides, attention imitation loss is only calculated on neurons in the TCDP, reducing the impact on the backdoor attack task. Second, attention transfer loss transfers the attention from one model to another for the same sample, while we achieve attention imitation across different samples. Specifically, the activation behavior of poisoned samples imitates that of benign samples with the target label. Therefore, it helps to evade defenses.

Formally, we define attention imitation loss ($\mathcal{A}I\mathcal{L}$) by Eq. 5,

$$\begin{aligned} \mathcal{A}I\mathcal{L} &= \sum_n^N \left\| \frac{\sigma_n(x', f')}{\|\sigma_n(x', f')\|_2} - \frac{\sigma_n(x_{ref}, f)}{\|\sigma_n(x_{ref}, f)\|_2} \right\|_1 \\ \mathcal{L}_2 &= \sum_{(x', y')}^{\mathcal{D}_{bd}[t]} \mathcal{A}I\mathcal{L}(x', x_{ref}, f', f) \end{aligned} \quad (5)$$

where $\sigma_n(\cdot, \cdot)$ denotes the activation value of the neuron n ; $\mathcal{D}_{bd}[t]$ denotes the set of samples with the target label t in the backdoored dataset \mathcal{D}_{bd} ; x' denotes a sample in $\mathcal{D}_{bd}[t]$; x_{ref} denotes a reference sample with the target label t , which is randomly selected from the clean dataset \mathcal{D}_c ; and f and f' denote the clean model and the backdoored model, respectively.

For each neuron n in the TCDP \mathcal{N} (see Section 4.4), $\mathcal{A}I\mathcal{L}$ first calculates the l_2 normalization of the activation values of x' in f' and x_{ref} in f on neuron n , respectively. Then, $\mathcal{A}I\mathcal{L}$ computes the l_1 normalization of their difference. Based on $\mathcal{A}I\mathcal{L}$, the loss function \mathcal{L}_2 of the attack enhancement task is computed over each sample in $\mathcal{D}_{bd}[t]$. As illustrated in Figure 3, $\mathcal{A}I\mathcal{L}$ plays two roles, one is for benign samples, and the other is for poisoned samples.

If $x' \in \mathcal{D}_{bd}^b$ (i.e., x' is a benign sample), $\mathcal{A}I\mathcal{L}$ guides its behavior in the backdoored model towards that in a clean model, as illustrated in the upper part of Figure 3. Specifically, due to the injection of the backdoor, the decision paths of x' in f' are prone to deviate. This deviation can be exploited for backdoor detection. $\mathcal{A}I\mathcal{L}$ assists in rectifying the deviated paths in f' to achieve survivability.

If $x' \in \mathcal{D}_{bd}^p$ (i.e., x' is a poisoned sample), $\mathcal{A}I\mathcal{L}$ forces poisoned samples and benign samples to behave similarly on the TCDP \mathcal{N} , as illustrated in the bottom part of Figure 3. This brings two distinct advantages. One advantage is to evade backdoor detection techniques such as gradient and activation map analysis, since benign samples and poisoned samples show similar behavior in f' . The other advantage is the tight coupling between the backdoor and the target class.

The intuition behind is that $\mathcal{A}I\mathcal{L}$ guides the decision path of poisoned samples partially overlaps with that of benign samples in the target class, thereby increasing the coupling degree between the backdoor and the classification accuracy of the target class. Additionally, the neurons in the TCDP \mathcal{N} are not only crucial for the classification of the target class, but part of them are also crucial for the classification of other classes (see Section 4.4), making the backdoor further coupled with the overall classification accuracy. Therefore, the backdoor becomes difficult for defense techniques to eliminate. Even if certain defense technique successfully eliminates the backdoor, it will inevitably lead to a significant decrease in the classification accuracy of benign samples. Ultimately, this renders defense techniques ineffective in mitigating the backdoor.

Optimized Binary-Task Training. We use the joint loss function in Eq. 3 to further train the micro-trained model f_m (see Section 4.3) into the enhanced backdoored model f' .

As shown by Eq. 3, we follow the common practice of multi-task learning to assign a weight ω_i to the loss of each task. By employing this approach, we are able to adjust the significance for each task manually. However, the fixed value of ω_i persists throughout the entire training process, which also has its limitations. Given that the two tasks can vary in their learning difficulty, they may exhibit differences in convergence rates and magnitudes. Specifically, as \mathcal{L}_2 is computed on a limited set of neurons, \mathcal{L}_2 exhibits a smaller scale and faster convergence rate compared to \mathcal{L}_1 . If \mathcal{L}_2 is close to convergence but \mathcal{L}_1 has not yet, the subsequent training process will shift towards the optimization direction of \mathcal{L}_1 . Consequently, f' will only find the local optimum, impacting the effectiveness of the \mathcal{L}_2 task. Therefore, the weight ω_i should be dynamic.

Previous work [4] adopts gradient normalization (Grad-Norm) to balance multiple tasks, which places gradient norms for different tasks on a common scale and dynamically adjusts gradient norms so that different tasks train at a similar rate. However, this strategy is not suitable for our training scenario as it may lead to an unstable training process and hinder model convergence. As shown in Figure 4, due to the extreme imbalance between the two tasks, ω_2 drops sharply and even becomes negative, while \mathcal{L}_2 fluctuates violently and quickly exceeds the calculable range.

Instead, we design a smoother cosine annealing strategy to achieve a better balance, which is surprisingly effective despite its simplicity, as illustrated in Figure 4. Algorithm 2 presents the detailed procedure of our optimized binary-task training. It first initializes the enhanced backdoored model f' as the micro-trained model f_m , and initializes ω_1 and ω_2 as 1 (Line 1-2). Then, it sets the maximum training steps T to adjust the weights (Line 3). The number of training steps for one epoch is obtained by dividing the size of the backdoored dataset \mathcal{D}_{bd} by the batch size $batch_size$, and T is the sum of this training steps for s epochs. This means that we adjust the weights of the two tasks within s epochs, which is similar to the effect of Grad-Norm [4]. Here, s is determined by the imbalance between the two tasks. The greater the imbalance, the smaller the value of s .

Next, Algorithm 2 updates the network f' to inject backdoor and enhance attack survivability by multiple steps (Line 4-15). At each step t , it first computes the loss of the two tasks, $\mathcal{L}_1(t)$ and $\mathcal{L}_2(t)$ (Line 5). Then, it balances the overall loss magnitudes by β (Line 9), otherwise the backdoor attack task will overwhelm the other task during the training [50]. The scaler β is computed in the first step

Algorithm 2 Optimized Binary-Task Training

Require: micro-trained model f_m , clean model f , clean dataset \mathcal{D}_c , backdoored dataset \mathcal{D}_{bd} , target class t , neurons in the TCDP \mathcal{N}

Ensure: enhanced backdoored model f'

```

1: Initialize the enhanced backdoored model  $f'$  as  $f_m$ 
2:  $\omega_1 \leftarrow 1, \omega_2 \leftarrow 1$ 
3:  $T \leftarrow s \cdot \frac{|\mathcal{D}_{bd}|}{batch\_size}$ 
4: for  $t = 0$  to  $total\_training\_steps$  do
5:   Input batch  $x_i$  to compute  $\mathcal{L}_1(t)$  and  $\mathcal{L}_2(t)$ 
6:    $\triangleright$  Adjust losses to a similar scale
7:   if  $t = 0$  then
8:      $\beta \leftarrow \frac{\mathcal{L}_1(0)}{\mathcal{L}_2(0)}$ 
9:      $\mathcal{L}_2(t) = \beta \cdot \mathcal{L}_2(t)$ 
10:     $\triangleright$  Use cosine annealing strategy to adjust weights
11:   if  $\omega_2 > 0.01$  then
12:      $\omega_2 \leftarrow \cos(\frac{\pi}{2} \cdot \frac{t}{T})$ 
13:      $\omega_1 \leftarrow 2 - \omega_2$ 
14:    $\mathcal{L}(t) \leftarrow \omega_1 \cdot \mathcal{L}_1(t) + \omega_2 \cdot \mathcal{L}_2(t)$ 
15:   Update the network  $f'$  to minimize  $\mathcal{L}(t)$ 

```

(Line 8). In each subsequent step, $\mathcal{L}_2(t)$ is scaled by multiplying it with β (Line 9). Next, it decays the weight ω_2 with a cosine annealing for each batch until ω_2 decreases to 0.01, and thereafter keeps it constant (Line 11-12). It also normalizes the two weights, ensuring that they add up to 2 (Line 13). Notice that this algorithm is suitable for scenarios where the two tasks are unbalanced.

5 EVALUATION

To evaluate the performance of VENOM, we design our evaluation to answer the following four research questions.

- **RQ1 Capability Preservation Evaluation:** How does VENOM preserve the capability of the original backdoor attacks?
- **RQ2 Survivability Evaluation:** How does VENOM enhance the survivability against model reconstruction-based defenses?
- **RQ3 Ablation Study:** What factors influence the performance of VENOM?
- **RQ4 Explainability Analysis:** What guarantees the performance of VENOM?

5.1 Evaluation Setup

We evaluate VENOM with two widely used DNN structures and three popular datasets. In our evaluation, we use VENOM to enhance eight backdoor attacks against eight backdoor defenses.

Models and Datasets. We select two DNNs (i.e., VGG19-BN [42] and PreActResNet18 [12]) and three datasets (i.e., CIFAR-10 [22], CIFAR-100 [22] and GTSRB [13]), which are widely used in backdoor literature. We use VGG19-BN for the three datasets, and PreActResNet18 for the CIFAR-10 dataset, achieving image classification tasks. Table 6 and 7 in Appendix A report details about datasets and models.

Attacks and Defenses. We use two criteria for selecting backdoor attack and defense techniques. First, it should be classic (e.g., the pioneer work) or advanced techniques (e.g., recently published work at top venues). Second, it should cover as many categories as possible within the taxonomy [25], aiming to demonstrate the effectiveness of VENOM against various types of attacks and defenses.

- **Backdoor Attack Selection.** We select eight backdoor attacks. Among them, BadNets [10], Blend [3] and TrojanNN [31] are classic poison-label visible attacks. LC [47] is a clean-label attack. SSBA [26] is a poison-based sample-specific invisible attack, while Inputaware [34] and WaNet [35] are training-controlled sample-specific attacks. Adap-Blend [37] is a recent attack which improves latent inseparability to bypass data distribution-based defenses. The general idea of each attack is introduced in Section 2.2.
- **Backdoor Defense Selection.** We select eight model reconstruction-based backdoor defenses. Among them, FT [29], NAD [28] and I-BAU [57] are model unlearning-based defenses. NC [53] is a trigger synthesis-based defense, which first synthesizes the trigger and then unlearns the backdoor. BNP [60], FP [29] and CLP [59] are model pruning-based defenses. NPD [62] attempts to block backdoor-related decision paths. The general idea of each defense is presented in Section 2.1.

VENOM Setup. For all image classification tasks, we follow the settings of the original attacks and defenses, and set the poison rate to 0.1 except for Adap-Blend where the poison rate is set to 0.003. During the training process, we use the SGD optimizer with a batch size of 128, a momentum of 0.9, and a weight decay of 5e-4. We set the initial learning rate to 0.01, and adopt a cosine annealing to set the learning rate for each training step during the whole epochs. The whole epochs are 80 on CIFAR-10 and CIFAR-100, and 60 on GTSRB.

For specific settings of VENOM, the micro-training step takes 5% of the whole epochs. In the TCDP generation step, we choose the last convolutional layer as the target layer, from which we select a total of 10 crucial neurons to form the TCDP; and we set the two thresholds ϵ_1 and ϵ_2 to 0.9 and 0.7. In the binary-task training step, we set s to 3 epochs. More details can be found in Appendix B.

Evaluation Metrics. As widely used in previous works, we also adopt *Benign Accuracy (BA)* and *Attack Success Rate (ASR)* to evaluate the utility and effectiveness of VENOM. In addition, we further propose *Attack Survivability Rate (ASuR)* to measure the impact of VENOM on enhancing attacks against defenses.

- **Benign Accuracy (BA).** BA is the accuracy of the backdoored model on the benign testing dataset. It is used to evaluate the utility of a backdoor attack. Besides, we use *Benign Accuracy Drop (BAD)* to measure the drop in BA of the backdoored model compared to the accuracy of the clean model. A lower BAD indicates that the backdoor attack has a lower impact on the model’s utility.
- **Attack Success Rate (ASR).** ASR is the ratio of the number of poisoned samples that are successfully attacked to the total number of poisoned samples in the testing dataset. It is used to measure the effectiveness of a backdoor attack.
- **Attack Survivability Rate (ASuR).** ASuR is a comprehensive metric that combines ASR and BA to assess the survivability of an attack against a defense. Existing defenses inevitably sacrifice a certain degree of BA while eliminating the backdoor [29]. Defenders typically set a lower limit of the BA drop, δ , to assess whether the defended model is acceptable. Prior works generally consider an effective defense to have a BA drop of no more than 10% [29, 54, 57], and thereby we set δ to -10%. After eliminating the backdoor via a defense, if BA still remains high (i.e., the BA drop is within the acceptable limit δ), defenders will believe that the model has been successfully defended and accept the defended model. In this case,

Table 1: Evaluation results of utility and effectiveness.

Attack	Original		VENOM-Enhanced		Original		VENOM-Enhanced	
	BA/BAD	ASR	BA/BAD	ASR	BA/BAD	ASR	BA/BAD	ASR
VGG19-BN + CIFAR-10								
BadNets	90.78/1.45	95.06	90.12/2.11	96.03	60.93/4.54	89.06	58.29/7.18	90.24
Blend	91.99/0.24	99.71	91.55/0.68	99.71	64.88/0.59	98.97	64.82/0.65	98.96
TrojanNN	91.44/0.79	100.00	91.85/0.38	99.99	65.00/0.47	99.99	65.77/-0.30	100.00
LC	83.48/8.75	99.46	83.52/8.71	99.82	65.58/-0.11	17.15	66.49/-1.02	55.76
SSBA	91.47/0.76	95.61	90.59/1.64	95.34	64.09/1.38	94.99	62.33/3.14	95.39
Inputaware	89.51/2.72	90.31	88.67/3.56	95.52	58.24/7.23	89.54	58.00/7.47	86.56
WaNet	85.17/7.06	99.09	85.45/6.78	98.47	55.13/10.34	98.45	50.73/14.74	98.05
Adap-Blend	92.10/0.13	71.90	92.07/0.16	70.12	68.49/-3.02	51.93	68.54/-3.07	71.44
Avg	89.49/2.74	93.89	89.23/3.00	94.38	62.79/2.68	80.01	61.87/3.60	87.05
VGG19-BN + GTSRB								
BadNets	97.49/0.63	94.81	97.97/0.15	95.34	91.41/2.42	94.78	89.94/3.89	95.90
Blend	97.85/0.27	99.94	98.36/-0.24	99.98	93.69/0.14	99.87	93.17/0.66	99.86
TrojanNN	98.09/0.03	100.00	98.35/-0.23	100.00	93.67/0.16	100.00	93.76/0.07	99.99
LC	97.82/0.30	63.03	97.65/0.47	63.74	84.95/8.88	93.36	85.18/8.65	92.14
SSBA	97.75/0.37	99.55	97.41/0.71	99.24	93.07/0.76	97.53	93.33/0.50	98.08
Inputaware	94.96/3.16	77.17	96.37/1.75	90.86	91.18/2.65	98.70	91.40/2.43	95.00
WaNet	94.78/3.34	98.12	94.84/3.28	93.83	90.12/3.71	85.99	90.05/3.78	96.91
Adap-Blend	97.21/0.91	70.54	96.48/1.64	71.11	93.68/0.15	74.63	93.10/0.73	74.28
Avg	96.99/1.13	87.90	97.18/0.94	89.26	91.47/2.36	93.11	91.24/2.59	94.02
PreActResNet18 + CIFAR-10								
BadNets	97.49/0.63	94.81	97.97/0.15	95.34	91.41/2.42	94.78	89.94/3.89	95.90
Blend	97.85/0.27	99.94	98.36/-0.24	99.98	93.69/0.14	99.87	93.17/0.66	99.86
TrojanNN	98.09/0.03	100.00	98.35/-0.23	100.00	93.67/0.16	100.00	93.76/0.07	99.99
LC	97.82/0.30	63.03	97.65/0.47	63.74	84.95/8.88	93.36	85.18/8.65	92.14
SSBA	97.75/0.37	99.55	97.41/0.71	99.24	93.07/0.76	97.53	93.33/0.50	98.08
Inputaware	94.96/3.16	77.17	96.37/1.75	90.86	91.18/2.65	98.70	91.40/2.43	95.00
WaNet	94.78/3.34	98.12	94.84/3.28	93.83	90.12/3.71	85.99	90.05/3.78	96.91
Adap-Blend	97.21/0.91	70.54	96.48/1.64	71.11	93.68/0.15	74.63	93.10/0.73	74.28
Avg	96.99/1.13	87.90	97.18/0.94	89.26	91.47/2.36	93.11	91.24/2.59	94.02

the smaller the drop in ASR compared to the undefended model, the stronger the survivability of the attack. Conversely, if BA becomes low (i.e., the BA drop exceeds δ), defenders will tend to not use the ineffective defense and still adopt the undefended model. In this case, the larger the drop in BA, the more likely to adopt the undefended model, and the stronger survivability of the attack; and meanwhile, the smaller the drop in ASR, the stronger the survivability of the attack. Overall, we expect the defended model either meets the effectiveness goal or fails to meet the utility goal. Based on this intuition, we define ASuR by Eq. 6.

$$\begin{aligned}
 \text{ASuR} &= \begin{cases} \alpha_1 \text{Scaler}(\Delta\text{ASR}) + \alpha_2 \text{Scaler}(\Delta\text{BA}) & , \text{if } \Delta\text{BA} \geq \delta \\ \alpha_1 \text{Scaler}(\Delta\text{ASR}) + \alpha_2 \text{Scaler}(-\Delta\text{BA}) & , \text{if } \Delta\text{BA} < \delta \end{cases} \\
 &= \begin{cases} 0.95\text{ASR}_a + 0.05 \frac{\Delta\text{BA} - \delta}{1 - \text{BA}_b - \delta} & , \text{if } \Delta\text{BA} \geq \delta \\ 0.50\text{ASR}_a + 0.50 \frac{\delta - \Delta\text{BA}}{\text{BA}_b + \delta} & , \text{if } \Delta\text{BA} < \delta \end{cases} \quad (6)
 \end{aligned}$$

where ΔASR and ΔBA respectively denote the drop in ASR and BA before and after a defense is applied. ASR_a and BA_b respectively denote the ASR after a defense is applied and the BA before a defense is applied. We employ Min-Max Scaler as the *Scaler*(\cdot) function. Specifically, when ΔBA is above δ , the drop in BA is usually considered as insignificant. Therefore, we set α_1 to 0.95 and α_2 to 0.05 to emphasize the drop in ASR. Here, $\Delta\text{BA} - \delta$ and $1 - \text{BA}_b - \delta$ represent the increase and maximum increase in BA, respectively. When ΔBA is below δ , we set α_1 to 0.50 and α_2 to 0.50 to comprehensively trade-off the drop in ASR and BA. Here, $\delta - \Delta\text{BA}$ and $\text{BA}_b + \delta$ represent the decrease and maximum decrease in BA, respectively. Therefore, a higher ASuR indicates a stronger survivability of an attack against a defense.

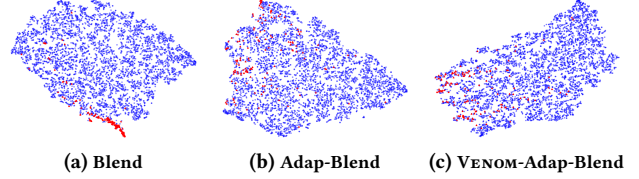
Environment. All our experiments were conducted on a Linux server with two 16-cores 32-threads Intel(R) Xeon(R) Silver 4314 CPUs as well as two NVIDIA GeForce RTX 3090 GPUs, running the Ubuntu 18.04.6 LTS x86_64 operating system.

5.2 Capability Preservation Evaluation (RQ1)

We use VENOM to enhance eight attacks, and evaluate how VENOM affects the capability of original attacks in terms of two aspects. First,

Table 2: Evaluation results of trigger stealthiness.

Attack	Original			VENOM-Enhanced		
	PSNR \uparrow	$I^\infty \downarrow$	LPIPS \downarrow	PSNR \uparrow	$I^\infty \downarrow$	LPIPS \downarrow
BadNets	27.308	169.792	0.0010	27.308	169.792	0.0010
Blend	20.655	47.969	0.0353	20.655	47.969	0.0353
TrojanNN	19.385	217.477	0.0431	19.385	217.477	0.0431
LC	24.465	204.027	0.0090	24.465	204.027	0.0090
SSBA	24.847	82.982	0.0139	24.847	82.982	0.0139
Inputaware	21.934	203.454	0.0687	21.906	200.111	0.0430
WaNet	31.164	45.164	0.0055	31.164	45.164	0.0055
Adap-Blend	21.019	48.844	0.0488	21.019	48.844	0.0488

**Figure 5: T-SNE visualization of latent inseparability. Benign and poisoned samples are respectively blue and red points.**

we measure VENOM’s impact on the utility and effectiveness by comparing the BA and ASR of the original attacks and VENOM-enhanced attacks. Second, we explore VENOM’s impact on the specific attack characteristics, i.e., trigger stealthiness and latent inseparability.

Utility and Effectiveness. Table 1 reports the BA, BAD and ASR of the original attacks and VENOM-enhanced attacks on the four classification tasks. On average, original attacks achieve a BAD of 2.23%, whereas VENOM-enhanced attacks have a BAD of 2.53%. Meanwhile, original attacks have an ASR of 88.73%, while VENOM-enhanced attacks achieve an ASR of 91.18%. Therefore, VENOM helps to slightly improve ASR by 2.45% at a cost of slight drop in BA by 0.30%.

Trigger Stealthiness. We use three widely used metrics, i.e., peak signal-to-noise ratio (PSNR) [15], I^∞ [23], and learned perceptual image patch similarity (LPIPS) [58], to measure the stealthiness of triggers. Table 2 shows the results of the original attacks and VENOM-enhanced attacks on VGG19-BN using CIFAR-10; and the results on the other three tasks are similar and thus are omitted. VENOM-enhanced attacks have almost the same trigger stealthiness as original attacks.

Latent Inseparability. Adap-Blend has a specific characteristic of latent inseparability that is missing from other attacks. Therefore, we analyze whether VENOM affects this characteristic. Figure 5 plots the latent representations of poisoned and benign samples for Blend, Adap-Blend and VENOM-enhanced Adap-Blend (i.e., VENOM-Adap-Blend) on VGG19-BN using CIFAR-10, visualized by T-SNE [49]; and the results on the other three tasks are similar and hence are omitted. Notable latent separation between benign and poisoned samples is observed for Blend, but the poisoned and benign samples mix with each other for both Adap-Blend and VENOM-Adap-Blend.

Moreover, we explore whether VENOM affects Adap-Blend’s resistance to four data distribution-based defenses, i.e., Spectral [46], AC [2], SCAN [44] and SPECTRE [11]. Table 3 presents the results on VGG19-BN using CIFAR-10; and the results on the other three tasks are similar and thereby are omitted. The columns *Eliminate* and *Sacrifice* respectively denote the ratio of poisoned samples that are eliminated and the ratio of benign samples that are mistakenly removed (i.e., sacrificed). Spectral and SPECTRE eliminate most of the poisoned samples with a negligible sacrifice of benign samples when

Table 3: Data distribution-based defenses against attacks.

Defense	Blend		Adap-Blend		VENOM-Adap-Blend	
	Eliminate	Sacrifice	Eliminate	Sacrifice	Eliminate	Sacrifice
Spectral	62.86	4.42	0.67	4.51	14.67	4.47
AC	0.00	0.00	1.33	3.17	0.00	0.00
SCAn	0.00	0.00	0.00	4.37	0.00	4.39
SPECTRE	86.47	0.23	0.00	0.45	0.00	0.45

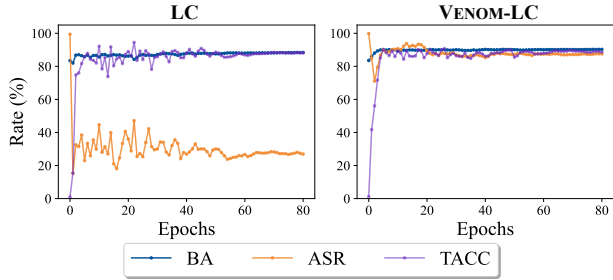


Figure 6: Defense process of FT against LC and VENOM-LC.

defending Blend. Differently, both Adap-Blend and VENOM-Adap-Blend evade all the four defenses with a low elimination rate of poisoned samples and a low sacrifice rate of benign samples.

Summary. VENOM preserves the capability of original attacks. In detail, VENOM keeps the utility, effectiveness and trigger stealthiness of original attacks, and also keeps the latent inseparability and the resistance to data distribution-based defenses of Adap-Blend.

5.3 Survivability Evaluation (RQ2)

We use eight defenses to defend the eight original attacks and eight VENOM-enhanced attacks, and investigate how VENOM enhances the attack survivability by comparing the BA, ASR and ASuR of the original and VENOM-enhanced attacks after the defenses are applied. As different defense follow different strategies, we conduct detailed analysis for different types of defenses respectively.

Results on VGG19-BN Using CIFAR-10. Table 4 reports the attack survivability comparison on VGG19-BN using CIFAR-10. After the defenses are applied, the original attacks still maintain a high BA (i.e., 88.70% on average), while their ASR drops to 41.76% averagely. Notably, 32.8% of the original attacks have an ASR that is lower than 10% after certain defenses are applied. On the contrary, the VENOM-enhanced attacks achieve an average BA of 88.18% and an average ASR of 71.03%. Notably, 39.1% of the VENOM-enhanced attacks have an ASR that is higher than 90% after certain defenses are applied. In that sense, VENOM enhances ASR by 29.27% with a slight decrease of BA by 0.52%. With respect to the comprehensive metric of ASuR, VENOM significantly enhances the attack survivability against various defenses, i.e., an average increase in ASuR from 41.12% to 69.73%.

Attack Survivability Against FT/I-BAU/NAD. As shown in Table 4, VENOM significantly reduces the effectiveness of these three model unlearning-based defenses, therefore enhancing the survivability of attacks in almost all configurations. Numerically, we observe an average increase in ASuR against FT by 43.40%, I-BAU by 25.60% and NAD by 35.18%. This is due to our tight coupling between the backdoor and the model’s classification performance.

Moreover, we take the LC attack against the FT defense as an example for a deeper insight. LC is a clean-label attack, and it causes the backdoored model to completely disregard the intrinsic features

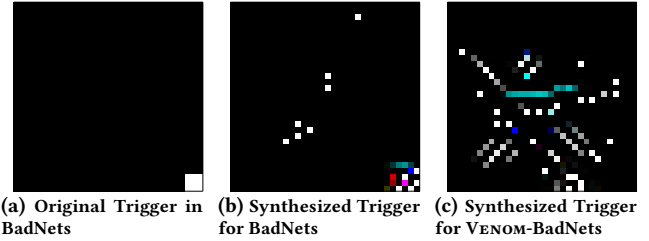


Figure 7: The original trigger in BadNets as well as NC’s synthesized triggers for BadNets and VENOM-BadNets.

of target-class samples and instead treat the trigger as the target class, thus sacrificing target-class accuracy (TACC) to ensure the success of the attack. Therefore, as shown by the defense process of FT in Figure 6, LC and VENOM-enhanced LC (i.e., VENOM-LC) have a very low TACC of 1.00% and 1.20% respectively, before FT is applied. FT aims to force the defended model’s attention back to the samples themselves, effectively rendering the backdoored model ineffective. In practice, as shown by the defense process of FT against LC, there is a decrease of ASR from 99.46% to 26.59% and an increase of BA from 83.48% to 88.51%, and TACC restores to a high value of 88.20%. However, as shown by the defense process of FT against VENOM-LC, as TACC increases, ASR exhibits only minor fluctuations before stabilizing at a high value of 85.72%. This result indicates that, due to the tight coupling between the backdoor and the model’s classification performance, repairing the model’s classification performance does not lead to the forgetting of the backdoor, instead, it actually helps to maintain the success of the attack.

Attack Survivability Against NC. As shown in Table 4, VENOM-enhanced attacks consistently maintain a high ASR after NC is applied. Specifically, only VENOM-BadNets and VENOM-Adap-Blend have an ASR around 70%, and the remaining VENOM-enhanced attacks achieve an ASR over 90%, which indicates the failure of NC. Compared to the original attacks, VENOM-enhanced attacks exhibit an average increase of 51.91% in ASR and 49.34% in ASuR.

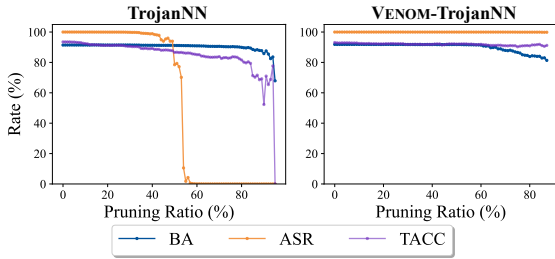
Besides, we take the BadNets attack against the NC defense as an example to show how VENOM evades NC. NC detects the poisoned target label, and synthesizes the trigger before eliminating the backdoor via model unlearning, and it requires that the synthesized trigger should be roughly similar to the original trigger (at least for BadNets) in terms of shape and location [53]. As shown in Figure 7, the synthesized trigger for BadNets appears to be similar to the original trigger, as both focus on the bottom-right corner of the image. However, the synthesized trigger for VENOM-BadNets differs significantly from the original trigger in terms of shape and location.

In fact, except for VENOM-BadNets and VENOM-LC, all VENOM-enhanced attacks evade the label detection in NC; i.e., NC considers the backdoored model as a clean model. Although NC correctly detects the poisoned label in VENOM-BadNets and VENOM-LC, it still fails to eliminate the backdoor because of the different shapes and locations between the synthesized and original triggers.

Attack Survivability Against FP/BNP/CLP/NPD. As shown in Table 4, VENOM significantly enhance ASuR against FP and NPD, achieving an increase of 34.09% and 31.23% respectively. While in the case of BNP and CLP, the enhancement is comparatively limited, with an ASuR increase of 5.84% and 4.28%, respectively. As most of the original attacks already exhibit high resistance against BNP, the

Table 4: Evaluation results of survivability on VGG19-BN using CIFAR-10 (O./V. denotes the original/VENOM-enhanced attack).

Defense	Metric	BadNets		Blend		TrojanNN		LC		SSBA		Inputaware		WaNet		Adap-Blend		Avg	
		O.	V.	O.	V.	O.	V.	O.	V.	O.	V.	O.	V.	O.	V.	O.	V.	O.	V.
FT	BA	88.80	90.30	89.82	90.81	89.61	89.95	88.51	90.37	89.50	90.38	91.33	90.63	91.36	91.27	90.87	91.99	89.98	90.71
	ASR	5.93	71.77	86.08	96.18	7.94	96.97	26.59	85.72	62.88	86.53	2.42	70.56	1.97	42.46	60.32	67.52	31.77	77.21
	ASuR	7.72	70.74	83.95	93.88	9.74	94.35	28.09	84.62	61.90	84.73	5.18	69.84	5.13	43.56	59.75	66.91	32.68	76.08
I-BAU	BA	85.34	89.41	86.45	86.48	85.84	88.61	86.55	86.89	87.66	88.80	88.93	88.24	89.12	89.58	90.48	89.87	87.55	88.48
	ASR	0.94	66.73	30.77	94.71	10.93	31.47	47.71	73.71	7.34	8.20	80.98	88.20	28.29	27.33	20.81	50.66	28.47	55.13
	ASuR	2.08	65.73	30.47	91.31	11.57	31.76	47.79	72.55	8.64	9.90	79.23	86.03	29.68	28.84	22.11	50.30	28.95	54.55
NAD	BA	88.15	89.62	88.16	90.54	88.45	88.88	87.20	89.91	88.93	90.22	90.99	90.35	91.01	91.23	90.73	91.45	89.20	90.28
	ASR	27.86	79.00	79.82	98.82	7.72	95.38	62.17	82.79	58.07	82.97	2.21	52.42	0.84	41.22	66.49	66.31	38.15	74.86
	ASuR	28.38	77.44	77.54	96.32	9.22	92.55	61.65	81.75	57.18	81.30	4.90	52.54	3.99	42.37	65.58	65.61	38.55	73.73
NC	BA	88.49	89.92	91.99	91.55	89.34	91.85	88.24	90.45	91.47	90.59	90.52	88.38	90.42	85.45	90.59	92.07	90.13	90.03
	ASR	14.19	67.73	99.71	99.71	6.32	99.99	30.43	91.79	95.61	95.34	2.91	93.47	0.39	98.47	51.84	70.12	37.67	89.58
	ASuR	15.49	66.81	97.50	97.43	8.13	97.75	31.69	90.40	93.53	93.15	5.45	91.07	3.44	95.58	51.62	69.40	38.36	87.70
FP	BA	89.06	90.14	90.17	90.51	89.79	89.86	89.26	90.64	89.12	90.05	91.43	90.49	90.99	91.42	91.36	91.81	90.15	90.61
	ASR	32.89	76.18	91.44	99.67	7.74	95.77	70.12	93.56	60.58	87.36	31.19	51.41	1.30	61.23	49.19	65.12	43.06	78.79
	ASuR	33.40	74.89	89.14	97.11	9.60	93.19	69.59	92.11	59.62	85.43	32.54	51.61	4.42	61.42	49.32	64.58	43.45	77.54
BNP	BA	90.10	89.66	91.17	90.73	90.38	91.23	83.05	83.08	90.98	90.24	90.00	84.81	66.79	25.94	91.22	91.73	86.71	80.93
	ASR	95.14	95.80	99.19	99.37	100.00	100.00	99.78	99.89	95.63	95.20	3.44	3.64	55.22	93.92	71.43	71.87	77.48	82.46
	ASuR	92.81	93.41	96.78	96.89	97.41	97.58	96.60	96.70	93.41	92.93	5.83	4.90	33.18	79.77	70.41	70.97	73.30	79.14
CLP	BA	89.11	73.11	87.09	89.78	89.01	90.95	81.31	82.28	89.49	82.97	89.86	84.81	71.37	86.43	91.63	88.02	86.11	84.79
	ASR	34.03	3.02	79.58	97.81	74.27	92.04	0.01	64.42	88.84	95.89	43.91	3.92	81.43	42.94	39.68	40.87	55.22	55.11
	ASuR	34.50	5.88	77.02	95.15	72.60	89.94	1.49	62.85	86.56	91.71	44.24	5.16	43.24	43.03	40.36	40.49	50.00	54.28
NPD	BA	90.11	89.92	90.92	90.84	91.40	91.16	86.46	87.23	89.96	90.00	88.49	87.77	89.73	88.71	90.99	91.44	89.76	89.63
	ASR	1.30	65.48	6.17	91.71	69.08	99.99	8.39	21.89	3.57	71.41	50.12	15.30	6.13	12.80	33.20	62.26	22.24	55.11
	ASuR	3.66	64.67	8.34	89.64	68.31	97.56	10.42	23.38	5.68	70.26	49.81	16.67	8.76	14.86	34.02	61.76	23.62	54.85
Avg	BA	88.64	87.76	89.47	90.16	89.23	90.31	86.32	87.61	89.64	89.16	90.19	88.19	85.10	81.25	90.98	91.05	88.70	88.18
	ASR	26.54	65.71	71.59	97.25	35.50	88.95	43.15	76.72	59.06	77.86	27.15	47.36	21.95	52.55	49.12	61.84	41.76	71.03
	ASuR	27.25	64.95	70.09	94.72	35.82	86.83	43.41	75.55	58.31	76.18	28.40	47.23	16.48	51.18	49.15	61.25	41.12	69.73

**Figure 8: Pruning process of FP against TrojanNN and VENOM-TrojanNN with respect to the pruning ratio.**

enhancement of VENOM is therefore limited in this particular case. Besides, VENOM fails to enhance the survivability of BadNets and Inputaware against CLP, leading to a limited ASuR improvement.

We take the TrojanNN attack against the FP defense as an example for a deeper investigation. FP eliminates the backdoor by pruning backdoor-related neurons of the selected layer. As illustrated by the pruning process of FP against TrojanNN and VENOM-TrojanNN in Figure 8, ASR of VENOM-TrojanNN remains around 100% even with a pruning ratio of 90%, but ASR of the original TrojanNN decreases significantly, with the backdoor completely eliminated when the pruning ratio reaches 60%. VENOM-enhanced attacks evade FP because VENOM embeds the backdoor into the neurons which are crucial for the classification of benign samples, rendering the decision path of poisoned samples overlapping with that of benign samples.

Results on the Other Three Tasks. For VGG19-BN on CIFAR-100, after the defenses are applied, VENOM helps existing attacks to averagely enhance ASR by 30.62% with an average decrease in BA of 0.24%. Overall, VENOM enhances the average attack survivability in

terms of ASuR from 32.91% to 61.85%. Consistently, for VGG19-BN on GTSRB, VENOM causes an average increase in attack survivability from 44.92% to 63.97%. For PreActResNet18 on CIFAR-10, VENOM increases the average attack survivability from 37.44% to 54.24%. Table 8, 9 and 10 in Appendix C report the detailed attack survivability comparison across attacks and defenses.

Summary. VENOM significantly enhances the original attacks’ survivability against model reconstruction-based defenses, leading to an average increase in ASuR from 39.10% to 62.45%.

5.4 Ablation Study (RQ3)

We evaluate the impact of several factors in the key TCDP generation step in VENOM, including the depth of the selected layer, the number of selected layers, and the number of selected neurons, on the survivability of VENOM-enhanced attacks. Further, we ablate each step in VENOM, i.e., micro-training, TCDP generation, and optimized binary-task training to measure the contribution of each step. We conduct all the experiments on VGG19-BN using CIFAR-10. For each attack, we report the average ASuR against eight defenses.

Impact of Layer Depth. We perform TCDP generation on each convolutional layer. However, the shallow layers have an empty TCDP, meaning that they are not directly crucial to target-class classification. Thus, we select the last four convolutional layers in the deep layers with the name of *features.40*, *features.43*, *features.46* and *features.49* (abbreviated as *f40*, *f43*, *f46* and *f49*), which contain at least 10 neurons in the generated TCDP. Figure 9(a) reports the impact of different layer depths on the average ASuR. Here we set the average ASuR of the original attacks as baselines. Overall, except for *f40* for VENOM-Inputaware and *f43* for VENOM-WaNet, the four

A general approach to enhance the survivability of backdoor attacks by decision path coupling

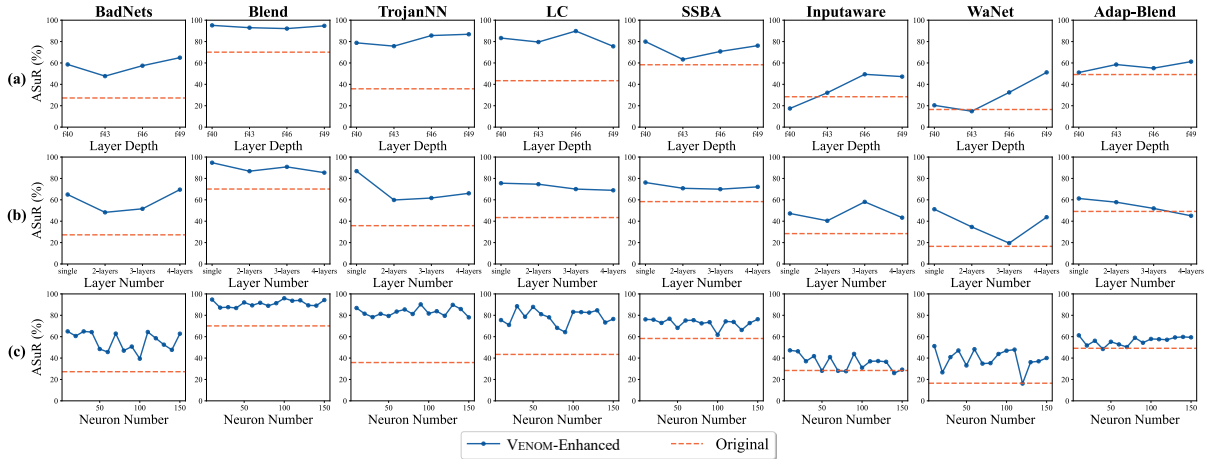


Figure 9: Impact of (a) layer depth, (b) layer number and (c) neuron number on the survivability of VENOM-enhanced attacks.

Table 5: Ablation analysis of different steps in VENOM.

Ablated Step	Bad-Nets	Blend	Trojan-NN	LC	SSBA	Input-aware	WaNet	Adap-Blend
Micro-Training	63.79	80.82	53.37	68.63	76.04	16.09	47.08	52.28
TCDP Generation	43.26	87.31	71.61	73.51	68.11	32.41	36.65	57.53
Optimized BTT	29.62	74.66	72.02	57.10	66.14	35.56	26.49	44.99
Full VENOM	64.95	94.72	86.83	75.55	76.18	47.23	51.18	61.25

layers all exhibit better ASuR than baselines, and as the layer depth increases, ASuR mostly has an increasing trend. Therefore, we use the last convolutional layer (i.e., f49) as the target single layer.

Impact of Layer Number. In TCDP generation, we select crucial neurons from one single layer. However, crucial neurons may be distributed across different layers. Hence, we conduct experiments on the single-layer setting and multi-layer settings. For the single-layer setting, we select f49 as the target single layer. For multi-layer settings, we use the above four deep layers to form paths of different lengths, i.e., f46-f49, f43-f46-f49 and f40-f43-f46-f49. Figure 9(b) illustrates the impact of different layer numbers on the average ASuR. As the layer number increases, ASuR mostly shows a declining trend. Compared to the single-layer setting, the average ASuR for the 2-layer setting decreases by 10.60%, with the 3-layer setting decreasing by 10.53% and the 4-layer setting by 7.96%. The intuition is that the gradients arising from different layers produce conflicting influences on the overall optimization, which hinders the finding of the global optimum. Therefore, we use the single-layer setting.

Impact of Neuron Number. We configure the number of selected neurons from 10 to 150 by a step of 10. Figure 9(c) shows the impact of different neuron numbers on the average ASuR. Except for some cases, most attacks exhibit similar performance across different numbers of selected neurons. Considering that more neurons bring higher computation complexity, we use 10 selected neurons.

Impact of Different Steps in VENOM. Table 5 reports the average ASuR of VENOM-enhanced attacks against eight defenses when each step of VENOM is ablated. First, we remove the micro-training step and initialize the backdoored model randomly. VENOM suffers a significant drop in ASuR on Blend, TrojanNN and Inputaware; and the average ASuR decreases by 10.30%. Second, we randomly select neurons from the target layer instead of selecting crucial neurons in the TCDP generation step. The average ASuR exhibits an decrease of

10.92%. Third, we remove our optimization in binary-task training (BTT) step, and set a fixed weight of 1 to ω_1 and ω_2 . The average ASuR decreases by 18.90% across all attacks. These results indicate the importance of each step in VENOM.

Summary. The layer depth, layer number and neuron number can affect the survivability of VENOM-enhanced attacks. Each step in VENOM contributes the performance of VENOM, with our optimization in binary-task training having the most contribution.

5.5 Explainability Analysis (RQ4)

We employ three DNN explainability techniques, i.e., Grad-CAM analysis, neuron activation analysis, and network feature analysis, to delve into the intrinsic mechanisms of VENOM. These techniques allow us to comprehend the decision-making process of the model from different dimensions, thus explaining the performance of VENOM.

Grad-CAM Analysis. Gradient-weighted Class Activation Mapping (Grad-CAM) [39] provides an intuitive visual explanation of the model’s decision-making process by generating heatmaps that reveal the key regions that the model focuses on. Grad-CAM is also frequently used in poisoned sample detection to localize trigger regions [5] without any prior knowledge of the attack. Here, we employ Grad-CAM to visualize how VENOM enhances BadNets and Inputaware, given that these two attacks employ visible local triggers which can be easily visualized by Grad-CAM.

As illustrated in Figure 10, Grad-CAM successfully localizes the trigger regions generated by the original BadNets and Inputaware attacks. However, when these attacks are equipped with VENOM, the key regions that contribute to the model’s classification decision for poisoned images shift from the trigger to the label object itself, hence making these attacks more stealthy and survivable.

Neuron Activation Analysis. Neuron activation analysis [38] examines the activation patterns of individual neurons or groups of neurons in response to different samples. It can gain insights into how specific parts of the model contribute to the decision-making process. Here, we explore the cosine similarity of activation values of the 10 crucial neurons between clean samples in the clean model and poisoned samples in the backdoored model, particularly analyzing the impact of VENOM on neuron activation behavior. Notice that

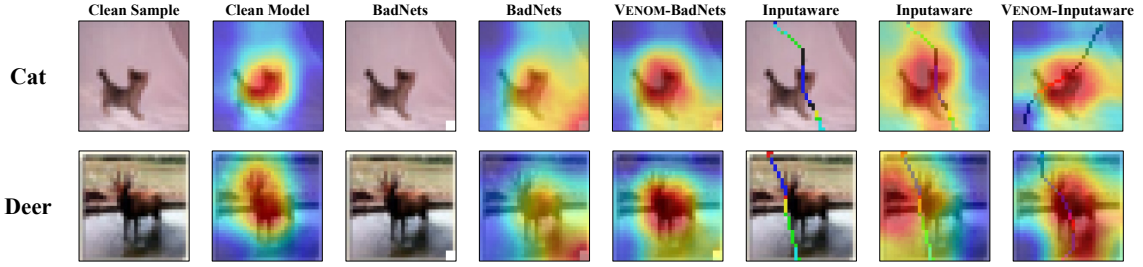


Figure 10: Grad-CAM visualization of the regions contributing to the model decision under BadNets and Inputaware.

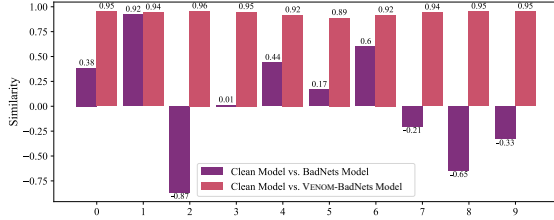


Figure 11: Similarity of crucial neuron activation between clean samples in clean model and poisoned samples in backdoored VGG19-BN model by BadNets and VENOM-BadNets.

these 10 neurons are considered as crucial for the model’s decision-making process, and if they exhibit different activation values from the clean model in the presence of backdoor, they can be the key for defenders to identify and eliminate the backdoor.

As shown in Figure 11, the backdoored model by BadNets has a relatively low similarity with the clean model in terms of the activation values of the 10 crucial neurons (i.e., denoted by the x -axis). Differently, the backdoored model by VENOM-BadNets achieves a very high similarity with the clean model. In other words, VENOM adjusts the neuron activation, forcing the model to process poisoned samples using the TCDP instead of using additional neurons. This not only allows the implanted features by the attacker in poisoned samples to be processed by the model similarly to clean samples, greatly enhancing the stealthiness and effectiveness of the attack, but also makes the backdoored model closer to the clean model in its internal representation, making it more difficult to detect and defend against.

Network Feature Analysis. Network feature analysis delves deeper into the model network, analyzing how the model extracts and utilizes features at different layers. By comparing the feature representations and their interactions at different layers, we can understand the contribution of each layer to the decision-making process. Here, we adopt Centered Kernel Alignment (CKA) [21] to quantify the similarity of representations between different layers.

As shown in Figure 12, the clean model and the backdoored models by BadNets and VENOM-BadNets exhibit some similarity in the shallow layers and the final linear layer. However, in the shallow layers of neural networks, models tend to learn generic, low-level visual features such as edges, textures, and colors. Hence, the shallow representations of different models are usually similar. For the final linear layer, all models aim to map high-level features into probability distributions, and thus they are also quite similar. However, for the deeper convolutional layers crucial for classification tasks (layers around the 45th layer), the backdoored model by BadNets shows significant differences from the clean model, which can be exploited

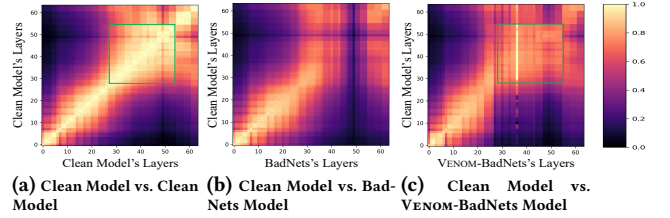


Figure 12: Comparison of network feature analysis between clean model and backdoored PreActResNet18 model by BadNets and VENOM-BadNets (with block structures highlighted).

by defenders. Hence, we choose the last convolutional layer as the target layer to implement VENOM, aiming to mitigate this difference.

Further, we observe the presence of *block structures* (i.e., many consecutive hidden layers that have highly similar representations [33]) in Figure 12(c), revealing similarity between the clean model and the backdoored model by VENOM-BadNets. Similar block structures also appear in Figure 12(a). Compared to the original BadNets as shown in Figure 12(b), VENOM-BadNets successfully enhances the backdoored model to exhibit similarity to the clean model in the TCDP. In addition, VENOM also achieves this similarity around the TCDP (i.e., the deeper convolutional layers) through forward and backward propagation during training, thereby enhancing the attack survivability.

Summary. The explainability techniques explain the rationality of the key designs in VENOM as well as the performance of VENOM.

6 DISCUSSION

Enhancing Poison-Only Attacks. Our threat model assumes that the attacker possesses control over the training process, and thus VENOM cannot be used to enhance poison-only attacks. It remains an open problem to enhance poison-only attacks’ survivability against model reconstruction-based defenses, e.g., how to poison the samples so that they have similar activation behaviors to benign ones.

Against Data Distribution-Based Defenses. Our work is solely focused on enhancing the survivability against model reconstruction-based defenses. However, as shown by Table 3 in Section 5.2, our experiments have demonstrated that Venom’s enhancement is independent of the original attack’s resistance against data distribution-based defenses. Therefore, the enhancements are combinable.

Generalized to Other Tasks. We focus on image classification tasks in this work, but VENOM can be applicable to other model architectures. Specifically, adapting the implementation for TCDP generation in different model structures is needed. Therefore, we believe that Venom can be generalized to other tasks, such as facial recognition and speech recognition. Our preliminary attempt on the face recognition task can be found in Appendix D.

Potential Defenses. Inspired by Differentially Private SGD [1] which adds noise to the gradient during the training process without affecting the final performance of the model and meanwhile protecting the privacy of the training data, one potential defense against VENOM is to apply a certain range of perturbations to model weights. As we assume that backdoor-related neurons are far less than the benign classification-related neurons, the backdoor is more sensitive to changes in model weights. Thus, the decision boundary of the perturbed backdoored model is unlikely to undergo significant shifts, thus preserving a high BA while exhibiting significant decrease in ASR. Nonetheless, the challenge remains formidable when it comes to effectively introducing perturbations to the model’s weights and precisely determining the optimal range for such perturbations.

7 CONCLUSIONS

We have proposed VENOM, the first generic approach to enhance the survivability of existing backdoor attacks against existing model reconstruction-based backdoor defenses. Our extensive evaluation has demonstrated the performance of tool. In future, we plan to evaluate VENOM on more tasks and develop defenses against VENOM.

REFERENCES

[1] Martin Abadi, Andy Chu, Ian Goodfellow, H Brendan McMahan, Ilya Mironov, Kunal Talwar, and Li Zhang. 2016. Deep learning with differential privacy. In *Proceedings of the 2016 ACM SIGSAC conference on computer and communications security*. 308–318.

[2] Bryant Chen, Wilka Carvalho, Nathalie Baracaldo, Heiko Ludwig, Benjamin Edwards, Taesung Lee, Ian Molloy, and Biplav Srivastava. 2018. Detecting backdoor attacks on deep neural networks by activation clustering. *arXiv preprint arXiv:1811.03728* (2018).

[3] Xinyun Chen, Chang Liu, Bo Li, Kimberly Lu, and Dawn Song. 2017. Targeted backdoor attacks on deep learning systems using data poisoning. *arXiv preprint arXiv:1712.05526* (2017).

[4] Zhao Chen, Vijay Badrinarayanan, Chen-Yu Lee, and Andrew Rabinovich. 2018. GradNorm: Gradient normalization for adaptive loss balancing in deep multitask networks. In *Proceedings of the International conference on machine learning*. 794–803.

[5] Edward Chou, Florian Tramèr, and Giancarlo Pellegrino. 2020. SentiNet: Detecting Localized Universal Attacks Against Deep Learning Systems. In *Proceedings of the 2020 IEEE Security and Privacy Workshops*. 48–54.

[6] Jacob Devlin, Ming-Wei Chang, Kenton Lee, and Kristina Toutanova. 2019. Bert: Pre-training of deep bidirectional transformers for language understanding. In *Proceedings of the 2019 Conference of the North American Chapter of the Association for Computational Linguistics: Human Language Technologies*. 4171–4186.

[7] Bao Gia Doan, Ehsan Abbasnejad, and Damith C Ranasinghe. 2020. Februus: Input purification defense against trojan attacks on deep neural network systems. In *Proceedings of the Annual computer security applications conference*. 897–912.

[8] Micah Goldblum, Dimitris Tsipras, Chulin Xie, Xinyun Chen, Avi Schwarzschild, Dawn Song, Aleksander Mądry, Bo Li, and Tom Goldstein. 2023. Dataset Security for Machine Learning: Data Poisoning, Backdoor Attacks, and Defenses. *IEEE Transactions on Pattern Analysis and Machine Intelligence* 45, 2 (2023), 1563–1580.

[9] Sorin Grigorescu, Bogdan Trasnea, Tiberiu Cocias, and Gigel Macesanu. 2020. A survey of deep learning techniques for autonomous driving. *Journal of Field Robotics* 37, 3 (2020), 362–386.

[10] Tianyu Gu, Kang Liu, Brendan Dolan-Gavitt, and Siddharth Garg. 2019. Badnets: Evaluating backdooring attacks on deep neural networks. *IEEE Access* 7 (2019), 47230–47244.

[11] Jonathan Hayase, Weihao Kong, Raghav Somani, and Sewoong Oh. 2021. Spectre: Defending against backdoor attacks using robust statistics. In *Proceedings of the International Conference on Machine Learning*. 4129–4139.

[12] Kaiming He, Xiangyu Zhang, Shaoqing Ren, and Jian Sun. 2016. Identity mappings in deep residual networks. In *Proceedings of the 14th European Conference on Computer Vision*. 630–645.

[13] Sebastian Houben, Johannes Stallkamp, Jan Salmen, Marc Schlipsing, and Christian Igel. 2013. Detection of traffic signs in real-world images: The German traffic sign detection benchmark. In *Proceedings of the 2013 International Joint Conference on Neural Networks*. 1–8.

[14] Kunzhe Huang, Yiming Li, Baoyuan Wu, Zhan Qin, and Kui Ren. 2021. Backdoor Defense via Decoupling the Training Process. In *Proceedings of the International*

Conference on Learning Representations.

[15] Quan Huynh-Thu and Mohammed Ghanbari. 2008. Scope of validity of PSNR in image/video quality assessment. *Electronics letters* 44, 13 (2008), 800–801.

[16] Sébastien Jean, Orhan Firat, and Melvin Johnson. 2019. Adaptive scheduling for multi-task learning. *arXiv preprint arXiv:1909.06434* (2019).

[17] Jinyuan Jia, Xiaoyu Cao, and Neil Zhenqiang Gong. 2021. Intrinsic certified robustness of bagging against data poisoning attacks. In *Proceedings of the AAAI Conference on Artificial Intelligence*. 7961–7969.

[18] Jinyuan Jia, Yupei Liu, Xiaoyu Cao, and Neil Zhenqiang Gong. 2022. Certified robustness of nearest neighbors against data poisoning and backdoor attacks. In *Proceedings of the AAAI Conference on Artificial Intelligence*. 9575–9583.

[19] Sara Kaviani and Insoo Sohn. 2021. Defense against neural trojan attacks: A survey. *Neurocomputing* 423 (2021), 651–667.

[20] Asifullah Khan, Anabia Sohail, Umme Zahoor, and Aqsa Saeed Qureshi. 2020. A survey of the recent architectures of deep convolutional neural networks. *Artificial intelligence review* 53, 8 (2020), 5455–5516.

[21] Simon Kornblith, Mohammad Norouzi, Honglak Lee, and Geoffrey Hinton. 2019. Similarity of neural network representations revisited. In *Proceedings of the International conference on machine learning*. 3519–3529.

[22] Alex Krizhevsky, Geoffrey Hinton, et al. 2009. Learning multiple layers of features from tiny images. (2009).

[23] Richard J Larsen and Morris L Marx. 2005. *An introduction to mathematical statistics*. Prentice Hall Hoboken, NJ.

[24] Alexander Levine and Soheil Feizi. 2020. Deep partition aggregation: Provable defense against general poisoning attacks. In *Proceedings of the International Conference on Learning Representations*.

[25] Yiming Li, Yong Jiang, Zhifeng Li, and Shu-Tao Xia. 2024. Backdoor learning: A survey. *IEEE Transactions on Neural Networks and Learning Systems* 35, 1 (2024), 5–22.

[26] Yuezun Li, Yiming Li, Baoyuan Wu, Longkang Li, Ran He, and Siwei Lyu. 2021. Invisible backdoor attack with sample-specific triggers. In *Proceedings of the IEEE/CVF international conference on computer vision*. 16463–16472.

[27] Yige Li, Xixiang Lyu, Nodens Koren, Lingjuan Lyu, Bo Li, and Xingjun Ma. 2021. Anti-backdoor learning: Training clean models on poisoned data. In *Proceedings of the Annual Conference on Neural Information Processing Systems*. 14900–14912.

[28] Yige Li, Xixiang Lyu, Nodens Koren, Lingjuan Lyu, Bo Li, and Xingjun Ma. 2021. Neural attention distillation: Erasing backdoor triggers from deep neural networks. In *Proceedings of the International Conference on Learning Representations*.

[29] Kang Liu, Brendan Dolan-Gavitt, and Siddharth Garg. 2018. Fine-pruning: Defending against backdooring attacks on deep neural networks. In *Proceedings of the International symposium on research in attacks, intrusions, and defenses*. 273–294.

[30] Risheng Liu, Jiabin Gao, Jin Zhang, Deyu Meng, and Zhouchen Lin. 2022. Investigating Bi-Level Optimization for Learning and Vision From a Unified Perspective: A Survey and Beyond. *IEEE Transactions on Pattern Analysis and Machine Intelligence* 44, 12 (2022), 10045–10067.

[31] Yingqi Liu, Shiqing Ma, Youssa Aafer, Wen-Chuan Lee, Juan Zhai, Weihang Wang, and Xiangyu Zhang. 2018. Trojaning attack on neural networks. In *Proceedings of the 25th Annual Network And Distributed System Security Symposium*.

[32] Yuntao Liu, Yang Xie, and Ankur Srivastava. 2017. Neural Trojans. In *Proceedings of the 2017 IEEE International Conference on Computer Design*. 45–48.

[33] Thao Nguyen, Maithra Raghu, and Simon Kornblith. 2020. Do Wide and Deep Networks Learn the Same Things? Uncovering How Neural Network Representations Vary with Width and Depth. In *Proceedings of the International Conference on Learning Representations*.

[34] Tuan Anh Nguyen and Anh Tran. 2020. Input-aware dynamic backdoor attack. In *Proceedings of the Annual Conference on Neural Information Processing Systems*. 3454–3464.

[35] Tuan Anh Nguyen and Anh Tuan Tran. 2021. WaNet-Imperceptible Warping-based Backdoor Attack. In *Proceedings of the International Conference on Learning Representations*.

[36] Omkar Parkhi, Andrea Vedaldi, and Andrew Zisserman. 2015. Deep face recognition. In *Proceedings of the 26th British Machine Vision Conference*.

[37] Xiangyu Qi, Tinghao Xie, Yiming Li, Saeed Mahloujifar, and Prateek Mittal. 2023. Revisiting the assumption of latent separability for backdoor defenses. In *Proceedings of the eleventh international conference on learning representations*.

[38] Archit Rathore, Nithin Chalapathi, Sourabh Palande, and Bei Wang. 2021. TopoAct: Visually exploring the shape of activations in deep learning. *Computer Graphics Forum* 40, 1 (2021), 382–397.

[39] Ramprasaath R. Selvaraju, Michael Cogswell, Abhishek Das, Ramakrishna Vedantam, Devi Parikh, and Dhruv Batra. 2017. Grad-CAM: Visual Explanations From Deep Networks via Gradient-Based Localization. In *Proceedings of the IEEE International Conference on Computer Vision*. 618–626.

[40] Soumyadip Sengupta, Jun-Cheng Chen, Carlos Castillo, Vishal M Patel, Rama Chellappa, and David W Jacobs. 2016. Frontal to profile face verification in the wild. In *Proceedings of the 2016 IEEE winter conference on applications of computer vision*. 1–9.

- [41] Reza Shokri et al. 2020. Bypassing backdoor detection algorithms in deep learning. In *Proceedings of the 2020 IEEE European Symposium on Security and Privacy*. 175–183.
- [42] K Simonyan and A Zisserman. 2015. Very deep convolutional networks for large-scale image recognition. In *Proceedings of the 3rd International Conference on Learning Representations*.
- [43] Christian Szegedy, Sergey Ioffe, Vincent Vanhoucke, and Alexander Alemi. 2017. Inception-v4, inception-resnet and the impact of residual connections on learning. In *Proceedings of the AAAI conference on artificial intelligence*. 4278–4284.
- [44] Di Tang, XiaoFeng Wang, Haixu Tang, and Kehuan Zhang. 2021. Demon in the variant: Statistical analysis of DNNs for robust backdoor contamination detection. In *Proceedings of the 30th USENIX Security Symposium*. 1541–1558.
- [45] Xiaoou Tang and Zhifeng Li. 2004. Frame synchronization and multi-level subspace analysis for video based face recognition. In *Proceedings of the 2004 IEEE Computer Society Conference on Computer Vision and Pattern Recognition*.
- [46] Brandon Tran, Jerry Li, and Aleksander Madry. 2018. Spectral Signatures in Backdoor Attacks. In *Proceedings of the Annual Conference on Neural Information Processing Systems*.
- [47] Alexander Turner, Dimitris Tsipras, and Aleksander Madry. 2019. Label-consistent backdoor attacks. *arXiv preprint arXiv:1912.02771* (2019).
- [48] Sakshi Udeshi, Shanshan Peng, Gerald Woo, Lionell Loh, Louth Rawshan, and Sudipta Chattopadhyay. 2022. Model agnostic defence against backdoor attacks in machine learning. *IEEE Transactions on Reliability* 71, 2 (2022), 880–895.
- [49] Laurens Van der Maaten and Geoffrey Hinton. 2008. Visualizing data using t-SNE. *Journal of machine learning research* 9, 11 (2008).
- [50] Simon Vandenhende, Stamatios Georgoulis, Wouter Van Gansbeke, Marc Proesmans, Dengxin Dai, and Luc Van Gool. 2021. Multi-task learning for dense prediction tasks: A survey. *IEEE transactions on pattern analysis and machine intelligence* 44, 7 (2021), 3614–3633.
- [51] Miguel Villarreal-Vasquez and Bharat Bhargava. 2020. Confoc: Content-focus protection against trojan attacks on neural networks. *arXiv preprint arXiv:2007.00711* (2020).
- [52] Binghui Wang, Xiaoyu Cao, Neil Zhenqiang Gong, et al. 2020. On certifying robustness against backdoor attacks via randomized smoothing. In *Proceedings of the Workshop on Adversarial Machine Learning in Computer Vision*.
- [53] Bolun Wang, Yuanshun Yao, Shawn Shan, Huiying Li, Bimal Viswanath, Haitao Zheng, and Ben Y Zhao. 2019. Neural cleanse: Identifying and mitigating backdoor attacks in neural networks. In *Proceedings of the 2019 IEEE Symposium on Security and Privacy*. 707–723.
- [54] Baoyuan Wu, Hongrui Chen, Mingda Zhang, Zihao Zhu, Shaokui Wei, Danni Yuan, and Chao Shen. 2022. Backdoorbench: A comprehensive benchmark of backdoor learning. In *Proceedings of the Annual Conference on Neural Information Processing Systems*. 10546–10559.
- [55] Pengfei Xia, Hongjing Niu, Ziqiang Li, and Bin Li. 2022. Enhancing backdoor attacks with multi-level mmd regularization. *IEEE Transactions on Dependable and Secure Computing* 20, 2 (2022), 1675–1686.
- [56] Sergey Zagoruyko and Nikos Komodakis. 2017. Paying More Attention to Attention: Improving the Performance of Convolutional Neural Networks via Attention Transfer. In *Proceedings of the 5th International Conference on Learning Representations*.
- [57] Yi Zeng, Si Chen, Won Park, Zhuoqing Mao, Ming Jin, and Ruoxi Jia. 2022. Adversarial Unlearning of Backdoors via Implicit Hypergradient. In *Proceedings of the International Conference on Learning Representations*.
- [58] Richard Zhang, Phillip Isola, Alexei A Efros, Eli Shechtman, and Oliver Wang. 2018. The unreasonable effectiveness of deep features as a perceptual metric. In *Proceedings of the IEEE conference on computer vision and pattern recognition*. 586–595.
- [59] Runkai Zheng, Rongjun Tang, Jianze Li, and Li Liu. 2022. Data-free backdoor removal based on channel lipschitzness. In *Proceedings of the European Conference on Computer Vision*. 175–191.
- [60] Runkai Zheng, Rongjun Tang, Jianze Li, and Li Liu. 2022. Pre-activation Distributions Expose Backdoor Neurons. In *Proceedings of the Annual Conference on Neural Information Processing Systems*. 18667–18680.
- [61] Nan Zhong, Zhenxing Qian, and Xinpeng Zhang. 2022. Imperceptible Backdoor Attack: From Input Space to Feature Representation. In *Proceedings of the Thirty-First International Conference on Artificial Intelligence*. 1736–1742.
- [62] Mingli Zhu, Shaokui Wei, Hongyuan Zha, and Baoyuan Wu. 2023. Neural polarizer: A lightweight and effective backdoor defense via purifying poisoned features. In *Proceedings of the Annual Conference on Neural Information Processing Systems*.

A DATASETS AND MODELS

Table 6 reports detailed information of the three datasets, including the number of classes, the size of the training and testing datasets,

Table 6: Details of datasets.

Datasets	Classes	Size (train/test)	Image Size
CIFAR-10 [22]	10	50,000/10,000	32×32
CIFAR-100 [22]	100	50,000/10,000	32×32
GTSRB [13]	43	39,209/12,630	32×32

Table 7: Models and their parameters.

Model	Training Dataset	Parameters	Accuracy
VGG19-BN [42]	CIFAR-10	139.62M	92.23%
	CIFAR-100	139.99M	65.47%
	GTSRB	139.76M	98.12%
PreActResNet18 [12]	CIFAR-10	11.17M	93.83%

and the size of the image. They are commonly employed in the evaluation of backdoor attacks [3, 10, 26, 47].

Table 7 provides detailed information of the DNN models. VGG19-BN and PreActResNet18 are implemented following the default configuration in Backdoorbench [54]. The benign accuracy of the four classification tasks are also presented in the last column, which serves as baselines for comparing the utility of backdoored models.

B ATTACK SETUP

We set the attack target to label 0 for all tasks. However, LC fails to inject backdoor into the model using the GTSRB dataset. The reason is that LC attack only poisons the target class, but the GTSRB dataset has only 210 images for class 0, which is insufficient for backdoor injection. Therefore, we set the attack target to label 1 for LC and VENOM-LC on the GTSRB dataset. As Adap-Blend partially stems from a low poison rate, we follow its original configuration to set its poison rate to 0.003 and its attack target on GTSRB to 2. Besides, the total epochs for most tasks are 80 epochs, but 60 epochs are already sufficient for the GTSRB dataset.

With respect to the specific setting of VENOM, the micro-training step takes 5% of the whole epochs, which is 4 epochs for CIFAR-10 and CIFAR-100 and 3 epochs for GTSRB. In the TCDP generation step, we uniformly select the last convolutional layer as the target layer to generate the target crucial decision path, i.e., *features.49* for VGG19-BN and *layer4.1.conv2* for PreActResNet18.

In the binary-task training step, we set s to 3 epochs. The value of s is related to the difficulty of the task. In our scenario, \mathcal{L}_2 drops quickly below 0.5 in the first few epochs, and thus we should set s to a small value to slow down the decline of \mathcal{L}_2 . After s epochs, \mathcal{L}_2 updates at a relatively slow rate, waiting for \mathcal{L}_1 to catch up and ultimately reaching a balance point.

C RESULTS ON THE OTHER THREE TASKS

Table 8 reports the attack survivability comparison on VGG19-BN using CIFAR-100. Compared to the original attacks, VENOM helps to increase ASR from 33.78% to 64.40% and ASuR from 32.91% to 61.85% on average. Specifically, the survivability enhancement on TrojanNN is particularly significant, with an average increase of 62.87% in ASuR, whereas in the case of WaNet, the enhancement is comparatively limited, with an average improvement of 8.56% in ASuR. From the perspective of defenses, VENOM generally enhances the resistance against various defenses. The resistance against NC shows the highest improvement, with an average increase of 46.58% in ASuR.

Table 8: Attack survivability comparison on VGG19-BN using CIFAR-100.

Defense	Metric	BadNets		Blend		TrojanNN		LC		SSBA		Inputaware		WaNet		Adap-Blend		Avg	
		O.	V.	O.	V.	O.	V.	O.	V.	O.	V.	O.	V.	O.	V.	O.	V.	O.	V.
FT	BA	59.06	60.17	61.83	64.81	61.22	65.58	63.23	66.54	60.40	62.78	64.06	62.70	64.46	62.35	63.62	68.11	62.23	64.13
	ASR	0.09	43.10	89.71	99.14	0.75	100.00	7.81	58.63	37.44	83.91	1.58	57.92	8.12	30.35	18.11	58.59	20.45	66.45
	ASuR	0.91	42.09	85.99	95.29	1.40	96.11	8.28	56.85	36.26	80.81	3.03	56.44	9.48	30.66	17.82	56.81	20.40	64.38
I-BAU	BA	56.27	57.77	57.41	62.76	59.29	63.37	58.38	63.04	56.24	61.38	61.00	62.70	60.82	59.94	62.79	65.84	59.02	62.10
	ASR	0.10	58.25	43.08	98.41	0.82	99.84	23.67	66.25	87.83	89.00	61.21	57.92	0.63	7.83	9.58	39.36	28.37	64.61
	ASuR	0.64	56.25	41.21	94.37	1.26	95.71	22.80	63.69	83.67	85.50	59.38	56.44	2.03	9.06	9.62	38.27	27.58	62.41
NAD	BA	57.84	59.93	59.44	64.57	59.00	64.53	63.63	66.42	57.80	62.02	63.43	62.22	63.88	61.85	62.53	67.71	60.94	63.66
	ASR	0.12	22.77	56.64	99.18	4.15	100.00	22.69	57.09	75.05	89.53	0.68	58.51	1.87	29.43	16.79	67.78	22.25	65.54
	ASuR	0.82	22.76	54.31	95.30	4.39	95.99	22.46	55.38	71.70	86.07	2.11	56.95	3.49	29.74	16.44	65.50	21.97	63.46
NC	BA	59.19	59.86	60.75	63.87	61.18	65.01	61.53	66.49	60.98	62.33	63.62	61.90	63.55	62.01	68.26	68.53	62.38	63.75
	ASR	0.28	24.67	0.01	99.04	1.01	99.98	4.40	55.76	57.01	95.39	0.96	43.75	0.33	16.59	51.81	71.09	14.48	63.28
	ASuR	1.11	24.56	0.66	95.09	1.65	96.03	4.85	54.12	54.91	91.67	2.40	42.90	1.99	17.56	50.40	68.74	14.75	61.33
FP	BA	61.05	60.19	63.37	64.57	63.58	65.37	64.82	66.54	62.88	61.90	63.67	61.83	64.63	62.63	66.59	68.78	63.83	63.98
	ASR	0.57	29.24	90.88	98.58	99.35	99.67	20.02	55.66	77.24	87.51	0.19	47.62	11.05	9.19	27.14	55.29	40.80	60.34
	ASuR	1.57	28.93	87.28	94.73	95.34	95.77	20.06	54.03	74.34	84.14	1.67	46.57	12.27	10.58	26.76	53.76	39.91	58.56
BNP	BA	60.35	58.40	64.77	64.65	63.90	65.77	64.94	66.28	63.38	58.41	58.82	58.00	50.60	15.21	67.14	64.51	61.74	56.40
	ASR	89.02	90.25	98.68	98.98	99.75	99.95	19.21	59.30	95.24	94.36	90.38	86.48	84.27	95.94	51.72	59.85	78.53	85.64
	ASuR	85.53	86.72	94.84	95.12	95.75	96.08	19.30	57.46	91.49	90.28	86.88	83.12	80.55	79.30	50.18	57.58	75.56	80.71
CLP	BA	56.91	25.67	59.16	62.49	56.83	61.51	62.87	64.57	57.42	46.82	49.46	33.40	58.95	50.72	53.27	64.60	56.86	51.22
	ASR	85.17	23.75	93.83	98.59	62.00	98.09	6.18	16.05	96.86	81.18	43.72	17.89	11.31	60.44	17.95	55.62	52.13	56.45
	ASuR	81.52	35.30	89.61	94.51	59.10	93.83	6.69	16.18	92.38	45.85	41.65	24.15	12.00	58.26	13.44	53.57	49.55	52.71
NPD	BA	60.51	58.40	62.01	62.51	62.12	63.64	63.60	64.49	61.73	61.43	60.75	59.67	60.34	58.84	66.18	67.48	62.15	62.06
	ASR	0.01	54.51	9.43	92.74	2.58	99.73	15.63	44.22	0.86	73.48	0.12	1.92	47.72	0.36	29.78	56.04	13.27	52.88
	ASuR	0.99	52.76	9.75	88.95	3.24	95.63	15.75	42.93	1.65	70.76	1.32	2.95	46.72	1.87	29.22	54.32	13.58	51.32
Avg	BA	58.90	55.05	61.09	63.78	60.89	64.35	62.88	65.55	60.10	59.63	60.60	57.80	60.90	54.19	63.80	66.94	61.15	60.91
	ASR	21.92	43.32	60.28	98.08	33.80	99.66	14.95	51.62	65.94	86.79	24.86	46.50	20.66	31.27	27.86	57.95	33.78	64.40
	ASuR	21.64	43.67	57.96	94.17	32.77	95.64	15.02	50.08	63.30	79.39	24.81	46.19	21.07	29.63	26.73	56.07	32.91	61.85

Table 9: Attack survivability comparison on VGG19-BN using GTSRB.

Defense	Metric	BadNets		Blend		TrojanNN		LC		SSBA		Inputaware		WaNet		Adap-Blend		Avg	
		O.	V.	O.	V.	O.	V.	O.	V.	O.	V.	O.	V.	O.	V.	O.	V.	O.	V.
FT	BA	97.74	97.85	97.78	98.23	98.34	98.31	97.81	98.12	97.84	97.50	97.80	97.27	98.34	98.42	95.83	96.77	97.69	97.81
	ASR	8.80	89.84	99.96	99.99	17.30	100.00	69.37	57.69	99.60	99.71	18.86	76.25	1.20	26.98	28.37	67.23	42.93	77.21
	ASuR	12.46	89.45	99.05	99.23	20.74	99.27	70.00	59.04	98.74	98.73	22.19	76.44	5.59	30.11	30.32	67.67	44.89	77.49
I-BAU	BA	96.85	97.34	96.48	97.32	24.23	96.85	5.29	97.59	96.61	96.71	95.73	95.87	97.19	97.73	85.65	94.83	74.75	96.78
	ASR	0.02	0.00	97.64	97.75	0.00	24.89	0.00	41.74	78.40	81.49	0.60	0.80	1.65	0.53	25.80	44.18	25.51	36.42
	ASuR	3.76	3.89	96.31	96.71	36.25	27.29	46.99	43.68	78.10	81.11	4.15	4.24	5.64	4.75	13.79	45.06	35.62	38.34
NAD	BA	97.56	98.04	97.73	98.27	98.14	98.12	97.79	98.00	97.70	97.44	97.62	97.20	98.20	98.47	95.84	96.54	97.57	97.76
	ASR	60.06	91.58	99.98	99.97	96.01	100.00	69.34	61.70	99.74	99.24	13.62	81.34	0.23	30.29	34.75	70.63	59.22	79.34
	ASuR	61.08	91.19	99.05	99.23	95.43	99.19	69.97	62.81	98.81	98.26	17.15	81.25	4.63	33.27	36.39	70.82	60.31	79.50
NC	BA	95.99	96.65	95.38	96.39	94.49	95.08	94.09	96.17	95.80	95.74	96.19	96.29	96.27	97.22	74.47	96.48	92.84	96.25
	ASR	0.01	95.06	67.68	81.23	32.08	100.00	25.21	44.51	46.68	91.75	65.23	0.21	0.29	10.86	49.77	71.11	35.87	61.84
	ASuR	3.41	93.91	67.39	80.62	33.16	97.89	26.52	45.73	47.63	90.47	65.70	3.84	4.05	14.40	32.19	71.25	35.01	62.26
FP	BA	97.81	98.07	97.95	98.31	98.41	98.10	97.74	98.30	98.09	97.50	97.55	97.24	98.24	98.57	95.74	96.71	97.69	97.85
	ASR	0.00	91.92	99.89	99.98	100.00	100.00	65.37	59.05	98.81	99.15	2.27	19.04	0.18	4.60	31.97	54.60	49.81	66.04
	ASuR	4.12	91.52	99.05	99.26	99.33	99.18	66.17	60.41	98.09	98.20	6.34	22.08	4.59	8.90	33.71	55.65	51.42	66.90
BNP	BA	97.43	97.95	97.83	98.41	98.17	98.29	97.72	97.55	97.59	97.48	95.67	94.43	13.39	89.09	75.24	96.46	84.13	96.21
	ASR	94.14	95.39	99.94	99.98	68.27	100.00	63.89	64.31	99.56	99.07	61.92	34.42	99.86	97.74	43.10	67.21	78.83	82.27
	ASuR	93.41	94.77	99.05	99.30	69.09	99.27	64.76	65.10	98.60	98.12	62.38	35.66	92.03	94.25	28.41	67.54	75.97	81.75
CLP	BA	97.54	97.74	97.33	98.19	97.82	97.56	96.99	97.68	97.35	96.30	95.96	96.45	76.45	35.99	74.34	96.52	91.88	89.62
	ASR	15.76	2.38	98.58	99.81	1.04	57.18	13.59	26.67	99.56	99.01	17.49	66.75	94.89	90.58	50.73	66.94	48.96	63.66
	ASuR	18.99	6.32	97.55	99.04	5.07	58.56	16.91	29.12	98.64	98.01	20.39	66.93	52.36	74.08	32.74	67.31	42.83	62.42
NPD	BA	97.19	96.64	97.40	97.14	95.41	96.69	96.68	97.18	96.98	96.94	96.55	95.34	97.02	96.37	84.48	95.73	95.21	96.50
	ASR	0.00	0.00	9.27	10.21	0.05	99.96	29.39	49.56	4.12	49.68	0.00	36.27	19.69	45.58	38.84	41.12	12.67	41.55
	ASuR	3.88	3.60	12.74	13.47	3.12	98.54	31.56	50.94	7.68	50.98	3.85	37.75	22.73	47.10	20.99	42.48	13.32	43.11
Avg	BA	97.26	97.53	97.23	97.78	88.13	97.46	85.59	97.49	97.29	97.08	96.68	96.20	84.39	88.98	85.20	96.25	91.47	96.10
	ASR	22.35	58.27	84.12	86.12	39.34	85.25	42.02	50.65	78.31</									

Table 10: Attack survivability comparison on PreActResNet18 using CIFAR-10.

Defense	Metric	BadNets		Blend		TrojanNN		LC		SSBA		Inputaware		WaNet		Adap-Blend		Avg	
		O.	V.	O.	V.	O.	V.	O.	V.	O.	V.	O.	V.	O.	V.	O.	V.	O.	V.
FT	BA	90.37	89.75	93.05	92.74	92.28	93.40	91.26	92.26	92.27	93.06	93.02	92.98	93.16	92.23	93.47	93.42	92.36	92.48
	ASR	1.73	75.10	95.04	98.52	3.82	3.19	35.56	49.57	80.64	94.52	73.41	95.20	15.32	35.13	71.18	76.82	47.09	66.01
	ASuR	4.05	73.79	93.16	96.44	6.27	6.00	37.04	50.53	79.33	92.71	72.89	93.55	17.83	36.43	70.62	76.03	47.65	65.69
I-BAU	BA	88.08	88.42	89.34	91.44	88.57	90.98	88.26	88.96	89.78	89.85	91.27	91.72	91.86	91.32	88.75	91.21	89.49	90.49
	ASR	2.19	1.76	8.63	53.30	1.86	3.54	11.61	21.04	6.21	28.08	0.17	31.24	2.01	62.50	16.40	47.39	6.13	31.11
	ASuR	3.87	3.79	9.93	53.09	3.27	5.59	13.69	22.76	7.88	28.63	2.84	32.45	4.86	62.20	17.13	47.42	7.93	31.99
NAD	BA	88.91	89.11	91.75	92.53	92.02	93.09	90.29	92.16	91.85	92.88	92.88	92.83	92.94	92.19	93.39	93.07	91.75	92.23
	ASR	1.21	49.20	76.56	97.52	2.26	3.07	20.44	43.57	85.49	92.56	10.29	97.14	8.46	45.44	66.49	74.82	33.90	62.91
	ASuR	3.17	49.03	75.20	95.42	4.70	5.79	22.48	44.81	83.81	90.80	12.88	95.36	11.26	46.21	66.14	74.03	34.95	62.68
NC	BA	89.63	89.35	92.33	92.84	93.67	93.76	89.78	85.18	92.38	93.09	92.82	91.15	92.28	92.18	93.68	93.22	92.07	91.35
	ASR	1.60	45.84	95.67	91.94	100.00	99.99	6.39	92.14	77.18	93.42	23.08	95.61	3.07	19.20	74.63	73.01	47.70	76.39
	ASuR	3.73	45.89	93.54	90.22	98.06	98.07	9.03	89.55	76.07	91.68	25.02	93.45	5.97	21.28	73.96	72.35	48.17	75.31
FP	BA	91.50	89.56	92.72	92.56	92.65	93.01	91.06	92.10	92.06	92.89	93.18	93.39	92.99	92.32	92.60	92.88	92.35	92.34
	ASR	0.90	44.20	25.87	65.10	64.51	97.64	55.02	65.28	14.86	51.08	10.36	68.72	1.86	3.64	37.12	42.71	26.31	54.80
	ASuR	3.57	44.39	27.34	64.63	64.03	95.61	55.48	65.42	16.77	51.39	13.03	68.51	5.00	6.53	38.00	43.47	27.90	54.99
BNP	BA	91.26	89.92	92.23	92.87	93.43	93.62	84.75	85.17	91.75	93.22	90.99	89.81	82.78	63.82	93.28	93.14	90.06	87.70
	ASR	94.26	95.83	99.73	99.89	100.00	99.99	94.49	92.62	97.72	97.87	2.11	2.21	25.23	99.08	75.37	75.83	73.61	82.92
	ASuR	92.20	93.53	97.36	97.78	97.99	98.03	91.72	90.00	95.40	95.94	4.61	4.36	24.64	59.68	74.54	75.01	72.31	76.79
CLP	BA	90.76	60.18	89.68	91.29	91.68	93.46	84.03	84.16	92.19	92.57	90.31	89.98	87.05	84.71	92.13	88.14	89.73	85.56
	ASR	14.59	8.02	99.21	98.50	98.24	99.99	2.01	10.41	98.00	96.21	3.03	38.60	13.82	25.24	67.22	22.08	49.51	49.88
	ASuR	16.38	16.37	96.09	95.99	95.78	97.98	3.72	11.70	95.79	94.17	5.30	38.98	14.87	25.15	66.45	22.47	49.30	50.35
NPD	BA	89.46	85.91	91.34	91.32	91.10	91.67	90.42	90.83	90.52	91.20	87.82	90.57	90.09	88.96	91.29	91.28	90.25	90.22
	ASR	0.26	0.74	12.77	16.81	34.89	7.69	14.01	32.80	5.08	13.67	1.41	0.03	0.42	1.47	6.40	42.66	9.41	14.48
	ASuR	2.41	2.19	14.48	18.39	35.42	9.74	16.40	34.31	7.03	15.35	3.10	2.49	2.91	3.63	8.41	42.95	11.27	16.13
Avg	BA	90.00	85.27	91.55	92.20	91.93	92.87	88.73	88.85	91.60	92.34	91.54	91.55	90.39	87.22	92.32	92.04	91.01	90.29
	ASR	14.59	40.09	64.19	77.70	50.70	51.89	29.94	50.93	58.15	70.93	15.48	53.59	8.77	36.46	51.85	56.91	36.71	54.81
	ASuR	16.17	41.12	63.39	76.49	50.69	52.10	31.20	51.13	57.76	70.08	17.46	53.64	10.92	32.64	51.91	56.72	37.44	54.24

from 44.23% to 63.54% and ASuR from 44.92% to 63.97%. Specifically, the survivability enhancement on BadNets and TrojanNN is significant, with an average improvement of 34.19% and 39.63% in ASuR respectively. From the perspective of defenses, VENOM generally enhances the resistance against various defenses. The resistance against FP shows the highest improvement, with an average increase of 32.60% in ASuR, whereas only Adap-Blend exhibits significantly enhanced resistance against I-BAU.

Table 10 provides the attack survivability comparison on PreActResNet18 using CIFAR-10. Generally, VENOM helps to improve the average ASR from 36.71% to 54.81% and ASuR from 37.44% to 54.24%. Specifically, the survivability enhancement on Inputaware is particularly significant, with an average improvement of 36.18% in ASuR, while in the case of TrojanNN, the enhancement is comparatively limited, with an average improvement of 1.41% in ASuR. From the perspective of defense, VENOM generally enhances the resistance against various defenses. Significant enhancement in resistance is observed for FP, NAD and NC, with all three exhibiting an average improvement around 27% in ASuR.

Of all the four tasks, VENOM exhibits the best enhancement on TrojanNN but the most limited enhancement on SSBA, with the average increase in ASuR by 38.87% and 14.30% on average. From the perspective of defenses, VENOM exhibits the best enhancement against NC but the most limited enhancement against BNP, with the average increase in ASuR by 37.58% and 5.31% on average. We observe that most original attacks already have significant resistance against BNP, leaving limited space for improvement.

Table 11: Attack survivability comparison between BadNets and VENOM-BadNets on InceptionResnetV1 using CFP.

Metric	No Defense		FP		FT	
	O.	V.	O.	V.	O.	V.
BA	92.00	91.53	90.00	88.73	95.00	92.60
ASR	83.00	87.71	11.00	75.82	3.00	41.22
ASuR	-	-	12.67	73.98	6.46	42.16

D RESULTS ON FACE RECOGNITION TASK

In addition to image classification tasks, we also apply VENOM to the face recognition task, where attackers confuse the model to recognize faces as a specific person and cause great harm. We select the InceptionResnetV1 model [43] and the CFP dataset [40]. CFP has 500 classes, and 5,000 and 2,000 training and testing samples of a size of 512×512. InceptionResnetV1 has 23.74M parameters, and achieves a benign accuracy of 100.00% on CFP. Our preliminary evaluation uses VENOM to enhance the attack survivability of BadNets against two defenses, i.e. FP and FT. Specifically, in the binary-task training step, we choose *repeat_3.4.conv2d* as the target layer to generate TCDP, and other settings follow the default one in Appendix B.

Table 4 reports the attack survivability comparison results. The original BadNets attack has little survivability against both defenses; i.e., ASR decreases from 83.00% to 11.00% and 3.00% respectively after FP and FT are applied, leading to a low ASuR of 12.67% and 6.46% respectively. As CFP contains 500 person, with only 14 images for each person, it is more prone to catastrophic forgetting, making FP and FT achieve a good defense capability against BadNets. However, the VENOM-enhanced BadNets still maintains a high ASR of 75.82% and 41.22% respectively, and exhibits an improved ASuR of 73.98%

A general approach to enhance the survivability of backdoor attacks by decision path coupling

and 42.16% respectively against the two defenses. This preliminary evaluation result has demonstrated the potential generalizability of VENOM to other tasks.

E ETHICS AND DATA PRIVACY

The training data used in our experiments are all from publicly available sources, serving solely for research purposes. All the experiments were conducted in a controlled environment, ensuring that no backdoored models were disseminated to model markets.